

Renormalisation group analysis of scalar Leptoquark couplings addressing flavour anomalies: emergence of lepton-flavour universality

Marco Fedele, Ulrich Nierste and Felix Wuest

*Institute for Theoretical Particle Physics, Karlsruhe Institute of Technology (KIT),
Wolfgang-Gaede-Str. 1, 76131 Karlsruhe, Germany*

E-mail: marco.fedele@kit.edu, ulrich.nierste@kit.edu,
felix.wuest@student.kit.edu

ABSTRACT: Leptoquarks with masses between 2 TeV and 50 TeV are commonly invoked to explain deviations between data and Standard-Model (SM) predictions of several observables in the decays $b \rightarrow c\tau\bar{\nu}$ and $b \rightarrow s\ell^+\ell^-$ with $\ell = e, \mu$. While Leptoquarks appear in theories unifying quarks and leptons, the corresponding unification scale M_{QLU} is typically many orders of magnitude above this mass range. We study the case that the mass gap between the electroweak scale and M_{QLU} is only populated by scalar Leptoquarks and SM particles, restricting ourselves to scenarios addressing the mentioned flavour anomalies, and determine the renormalisation-group evolution of Leptoquark couplings to fermions below M_{QLU} . In the most general case, we consider three SU(2) triplet Leptoquarks S_3^ℓ , $\ell = e, \mu, \tau$, which couple quark doublets to the lepton doublet (ν_ℓ, ℓ^-) to address the $b \rightarrow s\ell^+\ell^-$ anomalies. In this case, we find a scenario in which the Leptoquark couplings to electrons and muons are driven to the same infrared fixed point, so that lepton flavour universality emerges dynamically. However, the corresponding fixed point for the couplings to taus is necessarily opposite in sign, leading to a unique signature in $b \rightarrow s\tau^+\tau^-$. For $b \rightarrow c\tau\bar{\nu}$ we complement these with either an SU(2) singlet S_1^τ or doublet R_2^τ and study further the cases that also these Leptoquarks come in three replicas. The fixed point solutions for the S_3^ℓ couplings explain the $b \rightarrow s\ell^+\ell^-$ data for $S_3^{e,\mu}$ masses between 14 and 15 TeV, according to the scenario. $b \rightarrow c\tau\bar{\nu}$ data can only be fully explained by couplings exceeding their fixed-point values and evolving into Landau poles at high energies, so that one can place an upper bound on M_{QLU} between 10^8 and 10^{11} GeV.

KEYWORDS: Rare Decays, Semi-Leptonic Decays, Specific BSM Phenomenology

ARXIV EPRINT: [2307.15117](https://arxiv.org/abs/2307.15117)

Contents

1	Introduction	1
2	Effective Hamiltonians for B meson decays	3
3	Theory of leptoquarks	5
3.1	Lagrangians	6
3.1.1	Singlet leptoquarks	7
3.1.2	Doublet leptoquarks	8
3.1.3	Triplet leptoquarks	9
4	Renormalisation group equations	10
4.1	General results	10
4.2	The SM extended by S_1 and S_3 LQs	13
4.3	The SM extended by R_2 and S_3 LQs	14
5	Phenomenology of fixed point solutions	16
5.1	The (S_1, S_3) extension	17
5.2	The (R_2, S_3) extension	21
5.3	The S_3 extension	23
6	Conclusions	24

1 Introduction

Several measured branching ratios driven by the quark decay $b \rightarrow s\mu^+\mu^-$ show a deficit of events in the kinematic region with $q^2 \leq 8 \text{ GeV}^2$, where q^2 is the invariant mass of the lepton pair [1–3], if confronted with the Standard-Model (SM) prediction of refs. [4, 5]. Also the observable P'_5 parametrising an angular distribution in $B \rightarrow K^*\mu^+\mu^-$ follows this pattern [6–9].¹ In a 2022 reanalysis of LHCb data for the lepton flavour universality violating (LFUV) ratios [10]

$$R_{K^{(*)}} \equiv \frac{B(B \rightarrow K^{(*)}\mu^+\mu^-)}{B(B \rightarrow K^{(*)}e^+e^-)} \quad (1.1)$$

has resulted in values compatible with the SM predictions $R_{K^{(*)}} \simeq 1$ [11, 12]. Thus, while the previous results of $R_{K^{(*)}} \sim 0.8$ were hinting at the possibility of LFUV up

¹Refs. [4, 5] employ QCD sum rules, a method in which the contribution from excited hadrons to correlation functions is calculated perturbatively (“quark-hadron duality”). The uncertainty associated with this step is hard to quantify and critics suggested this as the source of the discrepancy.

to the 20% level, the current situation has strongly changed and violation of LFU is no longer preferred by data, although technically still allowed with reduced size. Therefore, if beyond-SM (BSM) physics is invoked to explain the $b \rightarrow s\mu^+\mu^-$, it will couple with similar strengths to muons and electrons.

Another long-standing flavour anomaly is related to $b \rightarrow c\tau\nu$ decays and observed in the ratios

$$R_{D^*} \equiv \frac{B(B \rightarrow D^{(*)}\tau\nu)}{B(B \rightarrow D^{(*)}\ell\nu)}, \quad \ell = e, \mu. \quad (1.2)$$

While BaBar and Belle have measured both ratios jointly, early LHCb measurements could only determine R_{D^*} . While all measurements have always been very consistent concerning R_{D^*} , there is some tension between the large 2012 BaBar value for R_D [13] and the corresponding 2019 Belle measurement with a smaller, SM-like result to the level expected by statistical fluctuation [14]. In 2022 LHCb has presented a combined $R_D - R_{D^*}$ measurement which has increased the overall consistency among all experimental results [15]. HFLAV combines six measurements [13–18] to [19]

$$R_D^{\text{exp}} = 0.358 \pm 0.025 \pm 0.012, \quad R_{D^*}^{\text{exp}} = 0.285 \pm 0.010 \pm 0.008, \quad (1.3)$$

which have to be compared with the SM predictions of [20–25]

$$R_D = 0.298 \pm 0.004, \quad R_{D^*} = 0.254 \pm 0.005, \quad (1.4)$$

entailing a discrepancy with eq. (1.3) of 3.2σ . Better measurements of D^* and τ polarisations can discriminate between different BSM explanations of $R_{D^{(*)}}$ [26, 27]. The ratio $R_{\Lambda_c} \equiv B(\Lambda_b \rightarrow \Lambda_c\tau\nu)/B(\Lambda_b \rightarrow \Lambda_c\ell\nu)$ contains redundant information to R_{D^*} in any model of New Physics (NP) [26, 27] and must move upward in future measurements from its 2022 value $R_{\Lambda_c}^{\text{LHCb}} = 0.242 \pm 0.026 \pm 0.040 \pm 0.059$ [28] to $R_{\Lambda_c} = 0.39 \pm 0.05$ [29] if $R_{D^{(*)}}^{\text{exp}}$ in eq. (1.3) are correct.

Leptoquarks (LQs) are the most popular particle species postulated to remedy the flavour anomalies. While giving an exhaustive list of references on this topic goes beyond the scope of this paper, a selection of the most prominent and innovative models involving LQs and addressing $b \rightarrow s$ and $b \rightarrow c$ anomalies can be found in refs. [30–43], and references therein. In this paper we focus on scalar LQs, which can be consistently added to the SM particle content. That is, their mass M_{LQ} is much below the scale M_{QLU} determining the masses of the remaining particles of some complete theory of quark-lepton unification (QLU) and the effects of the latter particles decouple for $M_{\text{QLU}} \rightarrow \infty$. By contrast, a vector LQ with mass $M_{\text{LQ}} \ll M_{\text{QLU}}$ corresponds to a non-decoupling scenario unless the Higgs sector responsible for its mass is taken into account as well. Flavour anomalies are addressed with the scalar LQs S_1 , R_2 and S_3 , denoting SU(2) singlet, doublet and triplet respectively, see figure 1 for sample diagrams. The combinations (S_1, S_3) or (R_2, S_3) can simultaneously cure $b \rightarrow c\tau\bar{\nu}$ and $b \rightarrow s\ell^+\ell^-$, with the caveat that one needs more than one copy of some SU(2) representations as explained below in section 3. The former scenario also affects the decay $b \rightarrow s\nu\bar{\nu}$ which is currently probed at the Belle II experiment. In both scenarios one can find large effects on the anomalous magnetic moment of the muon [44].

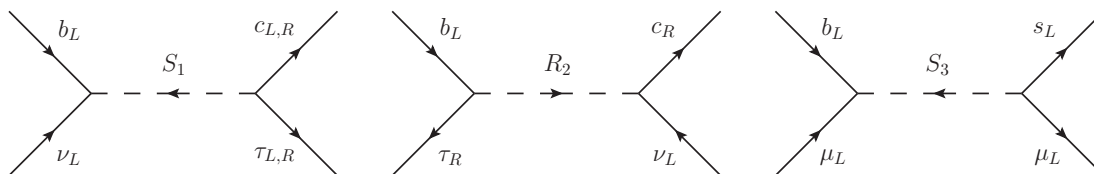


Figure 1. Contributions of scalar Leptoquarks to anomalous quark decays.

The presence of a sizable mass gap between M_{LQ} and M_{QLU} opens the possibility to study the renormalisation group (RG) to find generic predictions for the low-energy parameters without specifying details of the complete theory valid at M_{QLU} . The prototypical example for such a study is gauge coupling unification, which can be assessed from the SM beta functions alone, without knowing the parameters of the grand unified theory valid at the high scale. Indeed, the “near miss” of these running couplings nurtures the hope to find new particles in the reach of current particle colliders, because they change the slope of the beta functions. Another opportunity of RG analyses is the possibility to find infrared (IR) (quasi-) fixed points (FP) of parameters. Such studies have been pioneered in ref. [45] for the top Yukawa coupling, aiming at a prediction of the top mass. In this paper we derive and study the RG equations for LQ Yukawa couplings and SM gauge couplings.

The paper is organised as follows: in section 2 we report the effective Hamiltonians employed to describe B Meson decays in and beyond the SM, and summarize the current status of bounds on the NP couplings from the latest global fits. Section 3 reviews some basics and assesses the implications of low-energy data on the flavour pattern of the LQ Lagrangian. In section 4 we present the RG equations (RGE) of the LQ couplings first in a fully general theory and then specifically for the scenarios which can explain the flavour anomalies. Section 5 discusses the RGE FPs and their implications. Finally we conclude in section 6.

2 Effective Hamiltonians for B meson decays

It is customary to describe the decays of B mesons in the SM by means of effective field theories (EFTs), obtained after integrating out the top quark, the heavy gauge bosons Z and W , and the Higgs field. This approach is particularly helpful in the presence of BSM physics as well. Indeed, the low-scale footprints of any heavy degree of freedom can be parametrized at the B meson decay scale as shifts to the Wilson coefficients (WCs), describing the short-distance effects associated to all the fields integrated out of the theory. Therefore, after performing fits to all the available experimental data, it is possible to obtain bounds on the NP effects in a model independent way. These bounds can be then translated into constraints on any given model once the matching between the EFT and the desired BSM theory is performed. We will give the results of such matching for the relevant LQs in section 3.

The effective Hamiltonian employed to describe $b \rightarrow s\ell^+\ell^-$ transitions reads

$$\mathcal{H}_{\text{eff}}^{\ell\ell} \supset \frac{4G_F}{\sqrt{2}} V_{tb} V_{ts}^* (C_9^\ell \mathcal{O}_9^\ell + C_{10}^\ell \mathcal{O}_{10}^\ell) + \text{h.c.}, \quad (2.1)$$

where we focus on the phenomenologically relevant operators

$$\mathcal{O}_9^\ell = \frac{\alpha_{\text{em}}}{4\pi} (\bar{s}\gamma_\mu P_L b)(\bar{\ell}\gamma^\mu \ell), \quad \mathcal{O}_{10}^\ell = \frac{\alpha_{\text{em}}}{4\pi} (\bar{s}\gamma_\mu P_L b)(\bar{\ell}\gamma^\mu \gamma_5 \ell). \quad (2.2)$$

Here G_F is the Fermi constant, V_{tb} and V_{ts} are elements of the Cabibbo-Kobayashi-Maskawa (CKM) matrix, α_{em} is the fine structure constant and $P_{L,R} = (1 \mp \gamma_5)/2$. In the SM, the WCs are LFU and at the renormalization scale $\mu \equiv \mu_b = 4.8 \text{ GeV}$ equal to $C_9^\ell(\mu_b) \simeq 4.1$ and $C_{10}^\ell(\mu_b) \simeq -4.3$, respectively. It is also useful to define the quantity $C_L^\ell \equiv C_9^\ell = -C_{10}^\ell$.

As anticipated in the Introduction, the latest experimental results concerning $R_{K^{(*)}}$ [11, 12] require NP effects to be LFU, if one wants to address the discrepancies in $b \rightarrow s\mu^+\mu^-$ transitions by means of BSM physics. Defining therefore these additional contributions as $C_9^{\text{U}} \equiv C_9^e = C_9^\mu$ and $C_L^{\text{U}} \equiv C_L^e = C_L^\mu$, the most likely results found by the latest global fits [46–48] are

$$\begin{aligned} \text{I)} \quad & C_9^{\text{U}}(\mu_b) \sim -1, \\ \text{II)} \quad & C_L^{\text{U}}(\mu_b) \sim -0.4. \end{aligned} \quad (2.3)$$

As we will see in the next section, the WCs configuration found in scenario **II)** arises in the presence of S_3 LQs coupling equally to electron and muons.

It is interesting to notice that $b \rightarrow s\nu\bar{\nu}$ transitions can be described by an effective Hamiltonian closely related to the one given at eq. (2.1), namely

$$\mathcal{H}_{\text{eff}}^{\nu\bar{\nu}} \supset -\frac{4G_F}{\sqrt{2}} V_{tb} V_{ts}^* C_{\nu\bar{\nu}}^\ell \mathcal{O}_{\nu\bar{\nu}}^\ell + \text{h.c.}, \quad (2.4)$$

where we have introduced the neutrino operator

$$\mathcal{O}_{\nu\bar{\nu}}^\ell = \frac{\alpha_{\text{em}}}{4\pi} (\bar{s}\gamma_\mu P_L b)(\bar{\nu}\ell\gamma^\mu(1 - \gamma_5)\nu\ell). \quad (2.5)$$

Since experiment cannot distinguish neutrino flavours, the sum over all flavours appears in the ratio of the branching fraction and its SM prediction [49]:

$$R_{K^{(*)}}^{\nu\bar{\nu}} = \frac{\mathcal{B}^{\text{exp}}(B \rightarrow K^{(*)}\nu\bar{\nu})}{\mathcal{B}^{\text{SM}}(B \rightarrow K^{(*)}\nu\bar{\nu})} = \frac{(C_{\nu\bar{\nu}}^{\text{SM}} + C_{\nu\bar{\nu}}^e)^2 + (C_{\nu\bar{\nu}}^{\text{SM}} + C_{\nu\bar{\nu}}^\mu)^2 + (C_{\nu\bar{\nu}}^{\text{SM}} + C_{\nu\bar{\nu}}^\tau)^2}{3(C_{\nu\bar{\nu}}^{\text{SM}})^2}, \quad (2.6)$$

where $C_{\nu\bar{\nu}}^{\text{SM}}(\mu_b) \simeq -6.35$. On the one hand the current experimental limits in the K^* channel are set by the Belle collaboration [50], and read at 90% C.L. $R_{K^*}^{\nu\bar{\nu}} < 2.7$. On the other hand, concerning the K channel, the Belle II collaboration recently reported the first observation of this decay, which was found to be 2.8σ above its SM prediction [51], and corresponding to $R_K^{\nu\bar{\nu}} = 2.8 \pm 0.8$ when combined with previous measurements. In the case where NP couples to only one lepton flavour, these bounds imply at the 2σ level

$$-9 \lesssim C_{\nu\bar{\nu}}^{\text{NP}} \lesssim -1.7 \quad \cup \quad 14 \lesssim C_{\nu\bar{\nu}}^{\text{NP}} \lesssim 22, \quad (2.7)$$

where $C_{\nu\bar{\nu}}^{\text{NP}}$ represents any of $C_{\nu\bar{\nu}}^{e,\mu,\tau}$. An upcoming measurement by the Belle II collaboration in the $B \rightarrow K^* \nu\bar{\nu}$ channel is expected as well, which will provide further constraints on $C_{\nu\bar{\nu}}^{\text{NP}}$ [52].

The $b \rightarrow c\ell\nu$ transitions are described by the following effective Hamiltonian:

$$\mathcal{H}_{\text{eff}}^{\ell\nu} \supset \frac{4G_F}{\sqrt{2}} V_{cb} [(1 + C_{V_L}^\ell) \mathcal{O}_{V_L}^\ell + C_{S_L}^\ell \mathcal{O}_{S_L}^\ell + C_{S_R}^\ell \mathcal{O}_{S_R}^\ell + C_T^\ell \mathcal{O}_T^\ell] + \text{h.c.}, \quad (2.8)$$

where we have introduced the operators

$$\begin{aligned} \mathcal{O}_{V_L}^\ell &= (\bar{c}\gamma^\mu P_L b) (\bar{\ell}\gamma_\mu P_L \nu_\ell), & \mathcal{O}_{S_L}^\ell &= (\bar{c}P_L b) (\bar{\ell}P_L \nu_\ell), \\ \mathcal{O}_{S_R}^\ell &= (\bar{c}P_R b) (\bar{\ell}P_L \nu_\ell), & \mathcal{O}_T^\ell &= (\bar{c}\sigma^{\mu\nu} P_L b) (\bar{\ell}\sigma_{\mu\nu} P_L \nu_\ell), \end{aligned} \quad (2.9)$$

with $\sigma_{\mu\nu} = \frac{i}{2}[\gamma_\mu, \gamma_\nu]$. Given the normalization employed in eq. (2.8), all the WCs there appearing are describing genuine NP effects. It is worth to mention that in our study we will not consider effects coming from the operator \mathcal{O}_{V_R} , which is obtained by replacing P_L with P_R in the quark bilinear of \mathcal{O}_{V_L} , as it is LFU at dimension-six in the SMEFT [53–56]. Moreover, we do not allow for effects coming from right-handed neutrinos.

The latest bounds on the NP WCs involved in $b \rightarrow c\ell\nu$ transitions, both in a model-independent way and for specific UV models, can be found, e.g., in ref. [57]. As detailed in the following section, out of the several possible scenarios identified by the fit we focus here on the following scenarios, given at the renormalization scale μ_b :

$$\begin{aligned} \text{A)} & \quad C_{V_L}^T(\mu_b) \sim 0.08, \\ \text{B)} & \quad C_{S_L}^T(\mu_b) = -8.9C_T^T(\mu_b) \sim 0.19, \\ \text{C)} & \quad C_{S_L}^T(\mu_b) = 8.4C_T^T(\mu_b) \sim \pm i0.58. \end{aligned} \quad (2.10)$$

Scenarios **A)** and/or **B)** can arise in the presence of a S_1 LQ coupled to taus, while **C)** is instead a combination of WCs induced at the low scale by the presence of a R_2 LQ, coupling to taus.

3 Theory of leptoquarks

The updated LHCb values for $R_{K^{(*)}}$ [11, 12] imply that the NP interpretation of $b \rightarrow s\ell^+\ell^-$ data requires that both $b \rightarrow s\mu^+\mu^-$ and $b \rightarrow se^+e^-$ receive NP contributions with similar size [46–48]. As an immediate consequence, the S_3 LQ potentially mediating these decays must come in two copies, S_3^e and S_3^μ , each coupling only to the indicated lepton species. The reason why a single LQ cannot couple to both electrons and muons is the strong experimental bound on $\mu \rightarrow e$ conversion, which such a LQ would otherwise mediate. In the SM we observe an approximate $\text{SU}(2)^2$ flavour symmetry, corresponding to rotations of the charged right-handed fields (l_{1R}, l_{2R}) and the left-handed doublets (L_1, L_2) of the first two fermion generation. A priori the S_3 fields will couple to the weak eigenstates and the rotations of the latter into the flavour eigenstates $e_{L,R}$, $\mu_{L,R}$ (upon diagonalisation of the SM lepton Yukawa matrix) will lead to Leptoquarks coupling to both e and μ , which we must avoid. This rotation, however, is unphysical, if the LQ mass matrix is proportional

to the unit matrix, in which case one finds S_3^e and S_3^μ as desired. Mass-degenerate S_3^e and S_3^μ mean that the LQ mass term in the Lagrangian also obeys an SU(2) flavour symmetry related to rotations of leptons in flavour space.² Thus we conclude from the experimental evidence for $R_{K^{(*)}} \sim 1$ that Leptoquarks are part of the flavour puzzle and part (or even actors) of its explanation in term of approximate SU(2) symmetries.

For the $b \rightarrow c\tau\nu$ anomalies one may employ S_1 or R_2 exchange, see figure 1. For the former solution the S_1 coupling to $\bar{c}_L\tau_L^c$ comes with a coupling to $\bar{s}_L\nu_{\tau L}^c$ by SU(2) symmetry. This gives a large contribution to $b \rightarrow s\nu\bar{\nu}$, which could be mitigated by an S_3^e contribution of opposite sign in an appropriate model [38]. Therefore the (S_1, S_3) scenario could permit a significant enhancement of the branching ratio of $B \rightarrow K^{(*)}\nu\bar{\nu}$ currently studied at Belle II [51, 52]. The R_2 scenario can only successfully explain both $R(D)$ and $R(D^*)$ if the real part of the product of the $\bar{\tau}b_L$ and $\bar{c}\tau_R$ Yukawa couplings of R_2 is much smaller than the imaginary part (in the usual quark basis in which V_{cb} is real) [26, 27, 43, 58].

3.1 Lagrangians

Let us here review the formalism employed to describe scalar LQs. In order to do so, we adopt for fermion fields ψ the following formalism: $\psi_{L,R} = P_{L,R}\psi$, $\bar{\psi} = \psi^\dagger\gamma^0$ and $\psi^C = C\bar{\psi}^T$, where we have introduced $C = i\gamma^2\gamma^0$.

In the following we report the Lagrangians describing the interaction of scalar LQs with SM fields. We do not permit here diquark coupling of LQ, which would lead to dangerous and undesired proton decays [32], and do not consider LQs coupling to right-handed neutrinos. Hence, we will focus only on five families of scalar LQs, each denoted by different quantum numbers relatively to the SM gauge group (SU(3), SU(2), U(1)) [59]. In particular, we employ a fully general formalism, allowing in principle multiple copies for each LQ.

Before going into details for each LQ scenario we report here the generalization of the SM Yukawa Lagrangian to the case of n_H scalar Higgs doublets Φ^a , where $a = 1, \dots, n_H$, with generic flavour structure. These theories are usually defined as generic n_H Higgs doublet models (GNHDM), and can be described by the following Lagrangian:

$$\mathcal{L}_\Phi = -Y_{u,ij}^a \bar{Q}_{L,i}^l \epsilon^{lm} \Phi^{a,m} u_{R,j} - Y_{d,ij}^a \bar{Q}_{L,i} \Phi^a d_{R,j} - Y_{e,ij}^a \bar{L}_{L,i} \Phi^a e_{R,j} + \text{h.c.}, \quad (3.1)$$

where $\epsilon^{lm} = (i\tau^2)^{lm}$, with τ^2 being the second Pauli matrix. Moreover, $l, m = 1, 2$ are SU(2) indices and $i, j = 1, 2, 3$ are flavour indices. As stated above, we do not assume any particular flavour structure in the couplings among the several scalar Higgs doublets and the SM fields, namely each Higgs doublet Φ^a can couple with all SM fermions through the fully general coupling matrices $Y_{u,d,e}^a$.

Finally, we adopt the convention $g_1 \equiv \sqrt{3/5}g'$, $g_2 \equiv g$ and $g_3 \equiv g_s$, with g' , g and g_s being the U(1), SU(2) and SU(3) gauge couplings, respectively.

²We remark that such flavor symmetry forbids the presence of Higgs-mediated LQ self-interaction terms such as $(S_3^{e,\dagger} S_3^\mu)(\Phi^\dagger \Phi)$, which we therefore do not allow in our Lagrangians. Besides, contributions to the Yukawa RGE from self-interaction terms arises only at the two-loop level, hence beyond the scope of this paper.

3.1.1 Singlet leptoquarks

A scalar LQ $S_1 \equiv (\bar{\mathbf{3}}, \mathbf{1}, 1/3)$ interacts with the SM fields via the following Lagrangian:

$$\mathcal{L}_{\mathcal{Y}_{S_1}} = y_{1ij}^a \bar{Q}_{L,i}^C S_1^a \epsilon^{lm} L_{L,j}^m + x_{1ij}^a \bar{u}_{R,i}^C S_1^a e_{R,j} + \text{h.c.} \quad (3.2)$$

This Lagrangian describes all the coupling that are allowed for a weak singlet S_1 , which can couple either to two left-handed SM fermions, or to two right-handed ones. Similarly to the convention adopted for the Higgs doublets, here and below the index a is a family index employed to denote an arbitrary number of copies of a scalar LQ. This index can also be interpreted as a flavour index, analogously to the flavour indices i, j of the SM fermion fields. The interaction between an S_1^a LQ and the SM fields is mediated by arbitrary complex 3×3 Yukawa coupling matrices y_1^a and x_1^a , connected to left-handed and right-handed fermions respectively.

On the other hand, the interaction among a scalar LQ $\tilde{S}_1 \equiv (\bar{\mathbf{3}}, \mathbf{1}, 4/3)$ and SM fields is described by

$$\mathcal{L}_{\mathcal{Y}_{\tilde{S}_1}} = \tilde{x}_{1ij}^a \bar{d}_{R,i}^C \tilde{S}_1^a e_{R,j} + \text{h.c.} \quad (3.3)$$

Contrarily to S_1 in eq. (3.2), a weak singlet \tilde{S}_1 can only couple to two right-handed fields due to hypercharge conservation. This interaction is mediated by the arbitrary complex 3×3 Yukawa coupling matrix \tilde{x}_1^a .

The only scalar LQ which is going to be relevant for the phenomenological studies carried out in section 5 is S_1^τ , once non-vanishing values for the couplings y_{123}^τ , y_{133}^τ and x_{123}^τ are allowed. Indeed, it can contribute to $b \rightarrow c\tau\nu$ decays via [60]

$$C_{S_L}^\tau(\mu_{\text{LQ}}) = -4C_T^\tau(\mu_{\text{LQ}}) = -\frac{v^2}{4V_{cb}} \frac{y_{133}^\tau x_{123}^{\tau*}}{M_{S_1^\tau}^2}, \quad C_{V_L}^\tau(\mu_{\text{LQ}}) = \frac{v^2}{4V_{cb}} \frac{y_{133}^\tau (V_{cs} y_{123}^{\tau*} + V_{cb} y_{133}^{\tau*})}{M_{S_1^\tau}^2}, \quad (3.4)$$

at the matching scale $\mu_{\text{LQ}} = M_{S_1^\tau} \sim 2 \text{ TeV}$, with $v = 246 \text{ GeV}$. Notice that the relations among $C_{S_L}^\tau$ and C_T^τ is modified due to RGE effects once the coefficients are run down to the low scale, becoming $C_{S_L}^\tau(\mu_b) = -8.9 C_T^\tau(\mu_b)$ [61, 62]. It is worth mentioning that, due to SU(2) invariance, the presence of y_{133}^τ and y_{123}^τ implies a contribution to $b \rightarrow s\nu\bar{\nu}$ transitions as well, equal to [49]

$$C_{\nu\bar{\nu}}^\tau = \frac{\pi v^2}{V_{tb} V_{ts}^* \alpha_{\text{em}}} \frac{y_{133}^\tau y_{123}^{\tau*}}{m_{S_1^\tau}^2}. \quad (3.5)$$

Employing the results for scenarios **B**) or **A**) given in eq. (2.10) at the decay scale (which therefore take into account the running effects from $\mu_{\text{LQ}} = M_{S_1^\tau}$ to $\mu = \mu_b$) implies the following expected size for the NP parameters ratios, respectively:

$$\begin{aligned} \text{B)} \quad & \frac{y_{133}^\tau x_{123}^{\tau*}}{M_{S_1^\tau}^2} \sim -0.5 \text{ TeV}^{-2}, \\ \text{A)} \quad & \frac{y_{133}^\tau (V_{cs} y_{123}^{\tau*} + V_{cb} y_{133}^{\tau*})}{M_{S_1^\tau}^2} \sim 0.2 \text{ TeV}^{-2}. \end{aligned} \quad (3.6)$$

A few considerations are now in order. Starting from the $C_{S_L}^\tau = -4C_T^\tau$ scenario in eq. (3.4) one can infer that, for couplings of order unity, the LQ mass is of order $M_{S_1^\tau} \sim 1.5$ TeV. Even if y_{123}^τ is now assumed to be vanishing, we nevertheless obtain a vectorial contribution $C_{V_L}^\tau \propto V_{cb}y_{133}^\tau y_{133}^{\tau*}$, which is, however, negligible due to the CKM suppression: we are therefore consistent with scenario **B**) of eq. (2.10), where $C_{V_L}^\tau$ is assumed to be 0.

If, on the other hand, one would like to pursue the vectorial solution identified by scenario **A**) in eq. (2.10), a non-vanishing value for y_{123}^τ is required together with a vanishing x_{123}^τ , in order to remove the scalar/tensor WCs while evading CKM suppression in the vectorial one. In this scenario, coupling of order unity would imply for the LQ a mass of order $m_{S_1^\tau} \sim 3$ TeV. However, with this new choice of non-vanishing parameters a contribution for $C_{\nu\bar{\nu}}^\tau$ is implied as well, equal to ~ -130 and well above the current experimental bounds given at eq. (2.7). Such a scenario would therefore require some additional mechanism in order to avoid the $B \rightarrow K^{(*)}\nu\bar{\nu}$ bounds, like e.g. the one proposed in ref. [38].

3.1.2 Doublet leptoquarks

Moving on to weak doublets, the $R_2 \equiv (\mathbf{3}, \mathbf{2}, 7/6)$ scalar LQ Lagrangian is given by

$$\mathcal{L}_{\mathcal{Y}_{R_2}} = -y_{2ij}^a \bar{u}_{R,i} R_2^{a,l} \epsilon^{lm} L_{L,j}^m + x_{2ij}^a \bar{e}_{R,i} R_2^{a*} Q_{L,j} + \text{h.c.}, \quad (3.7)$$

Due to R_2 being a doublet, it can either couple to a left-handed lepton doublet and a right-handed quark singlet, or vice-versa. These interactions are mediated by the arbitrary complex 3×3 matrices y_2^a and x_2^a , respectively.

Similarly, the Lagrangian for $\tilde{R}_2 \equiv (\mathbf{3}, \mathbf{2}, 1/6)$ reads

$$\mathcal{L}_{\mathcal{Y}_{\tilde{R}_2}} = -\tilde{y}_{2ij}^a \bar{d}_{R,i} \tilde{R}_2^{a,l} \epsilon^{lm} L_{L,j}^m + \text{h.c.}. \quad (3.8)$$

Analogously to eq. (3.3), due to the different hypercharges of R_2 and \tilde{R}_2 only an interaction with a left-handed lepton doublet and a right-handed quark singlet is allowed for the latter, parameterized by the arbitrary complex 3×3 matrix \tilde{y}_2^a .

The doublet scalar R_2^τ LQ becomes phenomenologically relevant for us once the couplings y_{223}^τ and x_{233}^τ are allowed to be non-vanishing. Indeed, it contributes to $b \rightarrow c\tau\nu$ transitions via [60]

$$C_{S_L}^\tau(\mu_{\text{LQ}}) = 4C_T^\tau(\mu_{\text{LQ}}) = \frac{v^2}{4V_{cb}} \frac{y_{223}^\tau x_{233}^{\tau*}}{M_{R_2^\tau}^2}, \quad (3.9)$$

at the matching scale $\mu_{\text{LQ}} = M_{R_2^\tau} \sim 2$ TeV. Once again, due to RGE effects the relation among the coefficients reads $C_{S_L}^\tau(\mu_b) = 8.4C_T^\tau(\mu_b)$ at the low scale [61, 62]. The bound reported for scenario **C**) in eq. (2.10) can therefore be recast into a constraint on the parameter ratio

$$\frac{y_{223}^\tau x_{233}^{\tau*}}{M_{R_2^\tau}^2} \sim 1.5 \text{ TeV}^{-2}, \quad (3.10)$$

where we assumed one of the two coupling to be purely real and the other purely imaginary. Assuming for each coupling a size ~ 1 would imply a mass for the LQ below 1 TeV, already excluded by current constraints; it is however enough to require their size to be $\sim \sqrt{2}$, which is still below the current bounds obtained from searches for pair-produced LQs at

the LHC, to obtain a mass of the order $M_{R_2^c} \sim 1.7 \text{ TeV}$, heavy enough to evade present limits. See ref. [63] and references therein for a detailed discussion on the matter.

3.1.3 Triplet leptoquarks

We conclude this section describing the interactions among the weak triplet $S_3 \equiv (\bar{\mathbf{3}}, \mathbf{3}, 1/3)$ and the SM fields, ruled by the following Lagrangian:

$$\mathcal{L}_{\mathcal{Y}_{S_3}} = y_{3ij}^a \bar{Q}_{L,i}^{C,l} \epsilon^{lm} (\tau^k S_3^{a,k})^{mn} L_{L,j}^n + \text{h.c.}, \quad (3.11)$$

where τ^k are the Pauli matrices, with $k = 1, 2, 3$. The contraction $(\tau^k S_3^{a,k})$ can also be written as $(\vec{\tau} \cdot \vec{S}_3^a)$, as originally done in ref. [59]. Due to its triplet nature, S_3 LQs can couple only with two left-handed SM fermions through the arbitrary complex 3×3 matrix y_3^a , analogously to the first term of eq. (3.2).

The triplet LQ has relevant phenomenological implications on $b \rightarrow s\ell^+\ell^-$ transitions. Indeed, allowing non-vanishing values for the couplings $y_{33\ell}^\ell$ and $y_{32\ell}^\ell$, with $\ell = e, \mu \equiv 1, 2$, it is possible to obtain contributions of the form [60]

$$C_L^\ell(\mu_{\text{LQ}}) = \frac{\pi v^2}{V_{tb}V_{ts}^* \alpha_{\text{em}}} \frac{y_{33\ell}^\ell y_{32\ell}^{\ell*}}{M_{S_3}^2}, \quad (3.12)$$

at the matching scale $\mu_{\text{LQ}} = M_{S_3}^\ell$. Remembering that C_9 and C_{10} do not run in QCD, the result for scenario **II** in eq. (2.3) can be directly applied, and implies for the NP parameter ratio the value

$$\frac{y_{33\ell}^\ell y_{32\ell}^{\ell*}}{m_{S_3}^2} \sim 0.001 \text{ TeV}^{-2}. \quad (3.13)$$

Assuming the couplings to be of order unity, we can therefore infer the scale of the LQ mass to be $M_{S_3}^\ell \sim 30 \text{ TeV}$.

It is worth mentioning that, due to SU(2) invariance, allowing additional couplings to τ would induce contributions to $b \rightarrow c\tau\nu$ transitions as well, similar to the ones obtained for S_1 LQs. However, the sign of such contributions would be strictly negative due to additional constraints coming, e.g., from $\Delta_{m_{B_s}}$ [60] and hence not phenomenologically interesting, unless additional symmetries are imposed to the Lagrangian [38]. On the other hand, and again in a similar fashion to what is observed for the singlet LQ, contributions to $b \rightarrow s\nu\bar{\nu}$ transitions are unavoidable in this channel as well, and take the form

$$C_{\nu\bar{\nu}}^\ell = \frac{\pi v^2}{V_{tb}V_{ts}^* \alpha_{\text{em}}} \frac{y_{33\ell}^\ell y_{32\ell}^{\ell*}}{M_{S_3}^2}. \quad (3.14)$$

In this scenario, however, the induced size on $C_{\nu\bar{\nu}}^\ell$ from $b \rightarrow s\ell^+\ell^-$ data would correspond to $C_{\nu\bar{\nu}}^\ell \sim -0.6$. This value is well within the current bounds, even when allowing for NP coupled to two lepton families which imply a more stringent bound than the one given in eq. (2.7).

4 Renormalisation group equations

In this section we report the RGE of theories in which the SM sector is amended by an arbitrary number of Higgs doublets and scalar LQs. We start by giving in section 4.1 the RGEs for a fully generic theory with multiple copies of all the five scalar LQs. We then move to phenomenologically relevant cases, reporting the results obtained when the SM extended either with (S_1, S_3) LQs or with (R_2, S_3) LQs, in section 4.2 and section 4.3 respectively. All our results listed below correspond to the convention of our Lagrangians in eqs. (3.1)–(3.11). We give our results at the one-loop level of precision working in the $\overline{\text{MS}}$ -scheme, which we obtained adopting the findings of refs. [64, 65] to our specific scenarios.

RGE effects of couplings in theories with LQs have been studied before: recently, the two-loop RGEs for couplings have been derived including the necessary one-loop threshold corrections for the gauge and SM Yukawa couplings [66] and used to study coupling unification at high scales. Similarly, in ref. [67] two-loop RGEs were studied to assess perturbative unitarity and vacuum stability up to the Planck scale. Conversely, the authors of ref. [68] have studied the implications of an ultraviolet (UV) fixed point at the Planck scale, motivated by asymptotically safe gravity, on low-energy Leptoquark couplings. The couplings have been evolved to low energies and confronted with the flavour anomalies. While these papers employ RGEs to analyze UV properties of LQ theories, our study addresses the IR behaviour of LQ couplings. The RGE of gauge couplings was studied in refs. [47, 67] to check for Landau poles at high energies.

4.1 General results

Let us report here the RGE for the most general case, where arbitrary copies of the Higgs doublet and the five scalar LQs are allowed.

We start by giving the RGE for the gauge couplings g_1 , g_2 and g_3 , which we remember are connected to the U(1), SU(2) and SU(3) gauge couplings by the convention $g_1 \equiv \sqrt{3/5}g'$, $g_2 \equiv g$ and $g_3 \equiv g_s$. The RGE read

$$16\pi^2\mu\frac{d}{d\mu}g_1 = g_1^3\left(\frac{4}{3}n_f + \frac{1}{10}n_H + \frac{1}{15}n_{S_1} + \frac{16}{15}n_{\tilde{S}_1} + \frac{49}{30}n_{R_2} + \frac{1}{30}n_{\tilde{R}_2} + \frac{1}{5}n_{S_3}\right), \quad (4.1)$$

$$16\pi^2\mu\frac{d}{d\mu}g_2 = g_2^3\left(-\frac{22}{3} + \frac{4}{3}n_f + \frac{1}{6}n_H + \frac{1}{2}n_{R_2} + \frac{1}{2}n_{\tilde{R}_2} + 2n_{S_3}\right), \quad (4.2)$$

$$16\pi^2\mu\frac{d}{d\mu}g_3 = g_3^3\left(-11 + \frac{4}{3}n_f + \frac{1}{6}n_{S_1} + \frac{1}{6}n_{\tilde{S}_1} + \frac{1}{3}n_{R_2} + \frac{1}{3}n_{\tilde{R}_2} + \frac{1}{2}n_{S_3}\right), \quad (4.3)$$

where n_f represents the number of SM flavours, n_H is the number of scalar Higgs doublets, and n_{S_1} , $n_{\tilde{S}_1}$, n_{R_2} , $n_{\tilde{R}_2}$, n_{S_3} are the numbers of S_1 , \tilde{S}_1 , R_2 , \tilde{R}_2 , S_3 scalar LQs, respectively.

Before moving on to the RGE for the Yukawa couplings it is useful to define several quantities which will later allow us to state these RGE in a more compact and intuitive way. In particular, we give below the field renormalisation constants for all the relevant fields, namely the scalar Higgs doublets, the scalar LQs and the SM fermions.

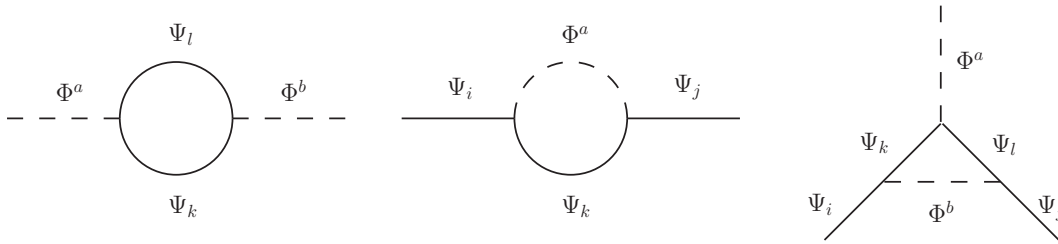


Figure 2. Diagrammatic representations of the contributions to the beta functions of the Yukawa couplings. Φ represents any scalar field, namely a Higgs doublet or a LQ, while Ψ represents any SM fermion field.

Starting from the six kind of scalars allowed in our theory, the contributions of the field renormalisation constants to the beta functions of the Yukawa couplings involve the following combinations of Yukawa matrices:

$$\begin{aligned}
 \mathbf{T}^{ab} &= \text{Tr} \left[N_c Y_u^{a\dagger} Y_u^b + N_c Y_d^{a\dagger} Y_d^b + Y_e^{a\dagger} Y_e^b \right], \\
 \mathbf{T}_1^{ab} &= \text{Tr} \left[2y_1^a y_1^{b\dagger} + x_1^a x_1^{b\dagger} \right], & \mathbf{T}_2^{ab} &= \text{Tr} \left[y_2^a y_2^{b\dagger} + x_2^a x_2^{b\dagger} \right], \\
 \tilde{\mathbf{T}}_1^{ab} &= \text{Tr} \left[\tilde{x}_1^a \tilde{x}_1^{b\dagger} \right], & \tilde{\mathbf{T}}_2^{ab} &= \text{Tr} \left[\tilde{y}_2^a \tilde{y}_2^{b\dagger} \right], & \mathbf{T}_3^{ab} &= \text{Tr} \left[2y_3^a y_3^{b\dagger} \right],
 \end{aligned} \tag{4.4}$$

where $N_c = 3$ is the colour number, and $a, b = 1, \dots, n_\alpha$ with $\alpha \in \{H, S_1, \tilde{S}_1, R_2, \tilde{R}_2, S_3\}$ is an index denoting possible multiple copies of each scalar. All terms in eq. (4.4) stem from diagrams involving fermion loops, like the left one in figure 2.

Concerning the field renormalisation constants of the SM fermion fields, we start with the contributions from loops with Higgs fields, which are

$$\begin{aligned}
 [\mathcal{Y}_Q]_{ij} &= \frac{1}{2} \left[Y_u^a Y_u^{a\dagger} + Y_d^a Y_d^{a\dagger} \right]_{ij}, & [\mathcal{Y}_L]_{ij} &= \frac{1}{2} \left[Y_e^a Y_e^{a\dagger} \right]_{ij}, \\
 [\mathcal{Y}_u]_{ij} &= \left[Y_u^{a\dagger} Y_u^a \right]_{ij}, & [\mathcal{Y}_d]_{ij} &= \left[Y_d^{a\dagger} Y_d^a \right]_{ij}, & [\mathcal{Y}_e]_{ij} &= \left[Y_e^{a\dagger} Y_e^a \right]_{ij},
 \end{aligned} \tag{4.5}$$

where we denote the (i, j) element of the matrix M by $[M]_{ij}$. Here and below, we adopt the convention that repeated indices are implicitly summed over.

The contribution for the fermion field renormalisations due to the insertion of LQ in a loop read

$$\begin{aligned}
 [\mathcal{Y}_1]_{ij} &= \frac{1}{2} \left[y_1^a y_1^{a\dagger} \right]_{ij}, & [\hat{\mathcal{Y}}_1]_{ij} &= \frac{N_c}{2} \left[y_1^{a\dagger} y_1^a \right]_{ij}, & [\mathcal{X}_1]_{ij} &= \frac{1}{2} \left[x_1^a x_1^{a\dagger} \right]_{ij}, \\
 [\mathcal{X}_1]_{ij} &= \frac{1}{2} \left[\tilde{x}_1^a \tilde{x}_1^{a\dagger} \right]_{ij}, & [\hat{\mathcal{X}}_1]_{ij} &= \frac{N_c}{2} \left[\tilde{x}_1^{a\dagger} \tilde{x}_1^a \right]_{ij}, & [\hat{\mathcal{X}}_1]_{ij} &= \frac{N_c}{2} \left[x_1^{a\dagger} x_1^a \right]_{ij}, \\
 [\mathcal{Y}_2]_{ij} &= \left[y_2^a y_2^{a\dagger} \right]_{ij}, & [\hat{\mathcal{Y}}_2]_{ij} &= \frac{N_c}{2} \left[y_2^{a\dagger} y_2^a \right]_{ij}, & [\mathcal{X}_2]_{ij} &= N_c \left[x_2^a x_2^{a\dagger} \right]_{ij}, \\
 [\mathcal{Y}_2]_{ij} &= \left[\tilde{y}_2^a \tilde{y}_2^{a\dagger} \right]_{ij}, & [\hat{\mathcal{Y}}_2]_{ij} &= \frac{N_c}{2} \left[\tilde{y}_2^{a\dagger} \tilde{y}_2^a \right]_{ij}, & [\hat{\mathcal{X}}_2]_{ij} &= \frac{1}{2} \left[x_2^{a\dagger} x_2^a \right]_{ij}, \\
 [\mathcal{Y}_3]_{ij} &= \frac{3}{2} \left[y_3^a y_3^{a\dagger} \right]_{ij}, & [\hat{\mathcal{Y}}_3]_{ij} &= \frac{3N_c}{2} \left[y_3^{a\dagger} y_3^a \right]_{ij}.
 \end{aligned} \tag{4.6}$$

Combining eq. (4.5) and eq. (4.6), both stemming from diagrams involving a fermion and a scalar in a loop as depicted in the center of figure 2, allows us to finally define the total contribution to the field renormalisations of the SM fermions, which read

$$\begin{aligned}
 [\mathcal{Y}_{QQ}]_{ij} &= [\mathcal{Y}_Q + \mathcal{Y}_1^* + \widehat{\mathcal{X}}_2 + \mathcal{Y}_3^*]_{ij}, & [\mathcal{Y}_{LL}]_{ij} &= [\mathcal{Y}_L + \widehat{\mathcal{Y}}_1 + \widehat{\mathcal{Y}}_2 + \widehat{\mathcal{Y}}_2 + \widehat{\mathcal{Y}}_3]_{ij}, \\
 [\mathcal{Y}_{uu}]_{ij} &= [\mathcal{Y}_u + \mathcal{X}_1^* + \mathcal{Y}_2]_{ij}, & [\mathcal{Y}_{dd}]_{ij} &= [\mathcal{Y}_d + \mathcal{X}_1^* + \mathcal{Y}_2]_{ij}, \\
 [\mathcal{Y}_{ee}]_{ij} &= [\mathcal{Y}_e + \widehat{\mathcal{X}}_1 + \widehat{\mathcal{X}}_1 + \mathcal{X}_2]_{ij},
 \end{aligned} \tag{4.7}$$

where the labels refer to the external fields.

Employing eq. (4.4) and eq. (4.7), complemented by additional contributions from vertex corrections as the one shown in the right side of figure 2, we are now ready to give the RGE for the Yukawa couplings introduced in section 3.1. The RGE of the SM Yukawa couplings defined in eq. (3.1) read

$$\begin{aligned}
 16\pi^2\mu\frac{d}{d\mu}[Y_u^a]_{ij} &= [Y_u^a]_{ij}\left(-8g_3^2 - \frac{9}{4}g_2^2 - \frac{17}{20}g_1^2\right) + \mathbf{T}^{ab*}[Y_u^b]_{ij} + [\mathcal{Y}_{QQ}]_{ik}[Y_u^a]_{kj} + [Y_u^a]_{ik}[\mathcal{Y}_{uu}]_{kj} \\
 &\quad - 2\left([Y_d^b Y_d^{a\dagger} Y_u^b]_{ij} - [y_1^b Y_e^a x_1^{b\dagger}]_{ij}^* + [y_2^b Y_e^a x_2^{b\dagger}]_{ij}\right),
 \end{aligned} \tag{4.8}$$

$$\begin{aligned}
 16\pi^2\mu\frac{d}{d\mu}[Y_d^a]_{ij} &= [Y_d^a]_{ij}\left(-8g_3^2 - \frac{9}{4}g_2^2 - \frac{1}{4}g_1^2\right) + \mathbf{T}^{ab}[Y_d^b]_{ij} + [\mathcal{Y}_{QQ}]_{ik}[Y_d^a]_{kj} + [Y_d^a]_{ik}[\mathcal{Y}_{dd}]_{kj} \\
 &\quad - 2[Y_u^b Y_u^{a\dagger} Y_d^b]_{ij},
 \end{aligned} \tag{4.9}$$

$$\begin{aligned}
 16\pi^2\mu\frac{d}{d\mu}[Y_e^a]_{ij} &= [Y_e^a]_{ij}\left(-\frac{9}{4}g_2^2 - \frac{9}{4}g_1^2\right) + \mathbf{T}^{ab}[Y_e^b]_{ij} + [\mathcal{Y}_{LL}]_{ik}[Y_e^a]_{kj} + [Y_e^a]_{ik}[\mathcal{Y}_{ee}]_{kj} \\
 &\quad + 2N_c\left([y_1^{b\dagger} Y_u^{a*} x_1^b]_{ij} - [x_2^b Y_u^a y_2^{b\dagger}]_{ij}\right).
 \end{aligned} \tag{4.10}$$

The RGE of the singlet LQs Yukawa couplings defined in eqs. (3.2)–(3.3) read

$$\begin{aligned}
 16\pi^2\mu\frac{d}{d\mu}[y_1^a]_{ij} &= [y_1^a]_{ij}\left(-4g_3^2 - \frac{9}{2}g_2^2 - \frac{1}{2}g_1^2\right) + \mathbf{T}_1^{ab}[y_1^b]_{ij} + [\mathcal{Y}_{QQ}]_{ik}^*[y_1^a]_{kj} + [y_1^a]_{ik}[\mathcal{Y}_{LL}]_{kj} \\
 &\quad + 2\left([Y_u^{b*} x_1^a Y_e^{b\dagger}]_{ij} - [x_2^{bT} x_1^{aT} y_2^b]_{ij}\right),
 \end{aligned} \tag{4.11}$$

$$\begin{aligned}
 16\pi^2\mu\frac{d}{d\mu}[x_1^a]_{ij} &= [x_1^a]_{ij}\left(-4g_3^2 - \frac{13}{5}g_1^2\right) + \mathbf{T}_1^{ab}[x_1^b]_{ij} + [\mathcal{Y}_{uu}]_{ik}^*[x_1^a]_{kj} + [x_1^a]_{ik}[\mathcal{Y}_{ee}]_{kj} \\
 &\quad + 4\left([Y_u^{bT} y_1^a Y_e^b]_{ij} - [y_2^{b*} y_1^{aT} x_2^b]_{ij}\right),
 \end{aligned} \tag{4.12}$$

$$16\pi^2\mu\frac{d}{d\mu}[\tilde{x}_1^a]_{ij} = [\tilde{x}_1^a]_{ij}\left(-4g_3^2 - 2g_1^2\right) + \tilde{\mathbf{T}}_1^{ab}[\tilde{x}_1^b]_{ij} + [\mathcal{Y}_{dd}]_{ik}^*[\tilde{x}_1^a]_{kj} + [\tilde{x}_1^a]_{ik}[\mathcal{Y}_{ee}]_{kj}. \tag{4.13}$$

The RGE of the doublet LQs Yukawa couplings defined in eqs. (3.7)–(3.8) read

$$16\pi^2\mu\frac{d}{d\mu}[y_2^a]_{ij} = [y_2^a]_{ij}\left(-4g_3^2 - \frac{9}{4}g_2^2 - \frac{5}{4}g_1^2\right) + \mathbf{T}_2^{ab}[y_2^b]_{ij} + [\mathcal{Y}_{uu}]_{ik}[y_2^a]_{kj} + [y_2^a]_{ik}[\mathcal{Y}_{LL}]_{kj} - 2\left([Y_e^b x_2^a Y_u^{b\dagger}]_{ij} + [x_1^{b*} x_2^{a*} y_1^b]_{ij}\right), \quad (4.14)$$

$$16\pi^2\mu\frac{d}{d\mu}[x_2^a]_{ij} = [x_2^a]_{ij}\left(-4g_3^2 - \frac{9}{4}g_2^2 - \frac{37}{20}g_1^2\right) + \mathbf{T}_2^{ab}[x_2^b]_{ij} + [\mathcal{Y}_{ee}]_{ik}[x_2^a]_{kj} + [x_2^a]_{ik}[\mathcal{Y}_{QQ}]_{kj} - 2\left([Y_u^b y_2^a Y_e^{b\dagger}]_{ij} + [y_1^{b*} y_2^{aT} x_1^b]_{ij}\right), \quad (4.15)$$

$$16\pi^2\mu\frac{d}{d\mu}[\tilde{y}_2^a]_{ij} = [\tilde{y}_2^a]_{ij}\left(-4g_3^2 - \frac{9}{4}g_2^2 - \frac{13}{20}g_1^2\right) + \tilde{\mathbf{T}}_2^{ab}[\tilde{y}_2^b]_{ij} + [\mathcal{Y}_{dd}]_{ik}[\tilde{y}_2^a]_{kj} + [\tilde{y}_2^a]_{ik}[\mathcal{Y}_{LL}]_{kj}. \quad (4.16)$$

Finally, the RGE of the triplet LQ Yukawa coupling defined in eq. (3.11) reads

$$16\pi^2\mu\frac{d}{d\mu}[y_3^a]_{ij} = [y_3^a]_{ij}\left(-4g_3^2 - \frac{9}{2}g_2^2 - \frac{1}{2}g_1^2\right) + \mathbf{T}_3^{ab}[y_3^b]_{ij} + [\mathcal{Y}_{QQ}]_{ik}^*[y_3^a]_{kj} + [y_3^a]_{ik}[\mathcal{Y}_{LL}]_{kj}. \quad (4.17)$$

4.2 The SM extended by S_1 and S_3 LQs

Let us now move our focus to the first of the two phenomenologically relevant models, whose RGE implications will be studied in section 5, namely the one consisting in the extension of the SM with S_1 and S_3 scalar LQs, and no additional Higgs doublets. This kind of models has been originally proposed in ref. [38] and subsequently embedded in a composite Higgs model in ref. [69]. They originally proposed a singlet LQ S_1 to account for the anomalies in $b \rightarrow c\tau\nu$ transitions, and a triplet LQ S_3 for addressing data in $b \rightarrow s\mu\mu$ decays, as shown in figure 1. As detailed in section 3, the requirement of lepton flavour universality in $b \rightarrow s\ell^+\ell^-$ transitions implies now the presence of multiple copies of S_3 LQs. While a similar behaviour is not required for the S_1 LQ, we will however maintain a degree of generality here and allow for multiple copies of this scalar LQ as well.

For this kind of theory eqs. (4.1)–(4.3) condense to

$$16\pi^2\mu\frac{d}{d\mu}g_1 = g_1^3\left(\frac{4}{3}n_f + \frac{1}{10} + \frac{1}{15}n_{S_1} + \frac{1}{5}n_{S_3}\right), \quad (4.18)$$

$$16\pi^2\mu\frac{d}{d\mu}g_2 = g_2^3\left(-\frac{22}{3} + \frac{4}{3}n_f + \frac{1}{6} + 2n_{S_3}\right), \quad (4.19)$$

$$16\pi^2\mu\frac{d}{d\mu}g_3 = g_3^3\left(-11 + \frac{4}{3}n_f + \frac{1}{6}n_{S_1} + \frac{1}{2}n_{S_3}\right). \quad (4.20)$$

The contribution from scalar field renormalisations are found from eq. (4.4), by specifying to only one Higgs doublet and SM Yukawas $Y_{u,d,e}^a \equiv Y_{u,d,e}$, and hence $\mathbf{T}^{ab} \equiv \mathbf{T}$. The fermion field renormalisations of eq. (4.7) are altered by the reduced scalar sector of the

theory, and now read

$$\begin{aligned}
 [\mathcal{Y}'_{QQ}]_{ij} &= [\mathcal{Y}_Q + \mathcal{Y}_1^* + \mathcal{Y}_3^*]_{ij}, & [\mathcal{Y}'_{LL}]_{ij} &= [\mathcal{Y}_L + \widehat{\mathcal{Y}}_1 + \widehat{\mathcal{Y}}_3]_{ij}, \\
 [\mathcal{Y}'_{uu}]_{ij} &= [\mathcal{Y}_u + \mathcal{X}_1^*]_{ij}, & [\mathcal{Y}'_{dd}]_{ij} &= [\mathcal{Y}_d]_{ij}, \\
 [\mathcal{Y}'_{ee}]_{ij} &= [\mathcal{Y}_e + \widehat{\mathcal{X}}_1]_{ij}.
 \end{aligned} \tag{4.21}$$

We have now all the ingredients necessary to give the RGE for the Yukawa couplings of an extension of the SM by multiple copies of S_1 and S_3 LQs. The RGE of the SM Yukawa couplings defined in eq. (3.1) read

$$\begin{aligned}
 16\pi^2\mu\frac{d}{d\mu}[Y_u]_{ij} &= [Y_u]_{ij}\left(-8g_3^2 - \frac{9}{4}g_2^2 - \frac{17}{20}g_1^2\right) + \mathbf{T}^*[Y_u]_{ij} + [\mathcal{Y}'_{QQ}]_{ik}[Y_u]_{kj} + [Y_u]_{ik}[\mathcal{Y}'_{uu}]_{kj} \\
 &\quad - 2\left([Y_d Y_d^\dagger Y_u]_{ij} - [y_1^b Y_e x_1^{b\dagger}]_{ij}^*\right),
 \end{aligned} \tag{4.22}$$

$$\begin{aligned}
 16\pi^2\mu\frac{d}{d\mu}[Y_d]_{ij} &= [Y_d]_{ij}\left(-8g_3^2 - \frac{9}{4}g_2^2 - \frac{1}{4}g_1^2\right) + \mathbf{T}[Y_d]_{ij} + [\mathcal{Y}'_{QQ}]_{ik}[Y_d]_{kj} + [Y_d]_{ik}[\mathcal{Y}'_{dd}]_{kj} \\
 &\quad - 2[Y_u Y_u^\dagger Y_d]_{ij},
 \end{aligned} \tag{4.23}$$

$$\begin{aligned}
 16\pi^2\mu\frac{d}{d\mu}[Y_e]_{ij} &= [Y_e]_{ij}\left(-\frac{9}{4}g_2^2 - \frac{9}{4}g_1^2\right) + \mathbf{T}[Y_e]_{ij} + [\mathcal{Y}'_{LL}]_{ik}[Y_e]_{kj} + [Y_e]_{ik}[\mathcal{Y}'_{ee}]_{kj} \\
 &\quad + 2N_c[y_1^{b\dagger} Y_u^* x_1^b]_{ij}.
 \end{aligned} \tag{4.24}$$

The RGE of the singlet LQs Yukawa couplings defined in eq. (3.2) read

$$\begin{aligned}
 16\pi^2\mu\frac{d}{d\mu}[y_1^a]_{ij} &= [y_1^a]_{ij}\left(-4g_3^2 - \frac{9}{2}g_2^2 - \frac{1}{2}g_1^2\right) + \mathbf{T}_1^{ab}[y_1^b]_{ij} + [\mathcal{Y}'_{QQ}]_{ik}^*[y_1^a]_{kj} + [y_1^a]_{ik}[\mathcal{Y}'_{LL}]_{kj} \\
 &\quad + 2[Y_u^* x_1^a Y_e^\dagger]_{ij},
 \end{aligned} \tag{4.25}$$

$$\begin{aligned}
 16\pi^2\mu\frac{d}{d\mu}[x_1^a]_{ij} &= [x_1^a]_{ij}\left(-4g_3^2 - \frac{13}{5}g_1^2\right) + \mathbf{T}_1^{ab}[x_1^b]_{ij} + [\mathcal{Y}'_{uu}]_{ik}^*[x_1^a]_{kj} + [x_1^a]_{ik}[\mathcal{Y}'_{ee}]_{kj} \\
 &\quad + 4[Y_u^T y_1^a Y_e]_{ij}.
 \end{aligned} \tag{4.26}$$

Finally, the RGE of the triplet LQ Yukawa coupling defined in eq. (3.11) reads

$$16\pi^2\mu\frac{d}{d\mu}[y_3^a]_{ij} = [y_3^a]_{ij}\left(-4g_3^2 - \frac{9}{2}g_2^2 - \frac{1}{2}g_1^2\right) + \mathbf{T}_3^{ab}[y_3^b]_{ij} + [\mathcal{Y}'_{QQ}]_{ik}^*[y_3^a]_{kj} + [y_3^a]_{ik}[\mathcal{Y}'_{LL}]_{kj}. \tag{4.27}$$

4.3 The SM extended by R_2 and S_3 LQs

The second phenomenologically relevant model consists of the extension of the SM with R_2 and S_3 scalar LQs, and again no additional Higgs doublets. This model was originally proposed in ref. [58] where the two LQs were embedded in an SU(5) Grand Unification Theory (GUT) and, as shown in figure 1, employs the R_2 LQ to address data in $b \rightarrow c\tau\bar{\nu}$ decays, again in combination with the S_3 LQ to explain anomalies in $b \rightarrow s\ell^+\ell^-$ transitions. Similarly to the previous case, we will permit multiple copies for both scalar LQs.

For this kind of model the gauge coupling RGE from eqs. (4.1)–(4.3) condense to

$$16\pi^2\mu\frac{d}{d\mu}g_1 = g_1^3\left(\frac{4}{3}n_f + \frac{1}{10} + \frac{49}{30}n_{R_2} + \frac{1}{5}n_{S_3}\right), \quad (4.28)$$

$$16\pi^2\mu\frac{d}{d\mu}g_2 = g_2^3\left(-\frac{22}{3} + \frac{4}{3}n_f + \frac{1}{6} + \frac{1}{2}n_{R_2} + 2n_{S_3}\right), \quad (4.29)$$

$$16\pi^2\mu\frac{d}{d\mu}g_3 = g_3^3\left(-11 + \frac{4}{3}n_f + \frac{1}{3}n_{R_2} + \frac{1}{2}n_{S_3}\right), \quad (4.30)$$

In a similar fashion to the previous scenario, the scalar field renormalisations are analogous to the ones given at eq. (4.4) specified to a single Higgs doublet, while for the fermion ones we now have

$$\begin{aligned} [\mathcal{Y}''_{QQ}]_{ij} &= [\mathcal{Y}_Q + \widehat{\mathcal{X}}_2 + \mathcal{Y}_3^*]_{ij}, & [\mathcal{Y}''_{LL}]_{ij} &= [\mathcal{Y}_L + \widehat{\mathcal{Y}}_2 + \widehat{\mathcal{Y}}_3]_{ij}, \\ [\mathcal{Y}''_{uu}]_{ij} &= [\mathcal{Y}_u + \mathcal{Y}_2]_{ij}, & [\mathcal{Y}''_{dd}]_{ij} &= [\mathcal{Y}_d]_{ij}, \\ [\mathcal{Y}''_{ee}]_{ij} &= [\mathcal{Y}_e + \mathcal{X}_2]_{ij}. \end{aligned} \quad (4.31)$$

We can now move on to the RGE equations for the Yukawa couplings in this kind of theory. The RGE of the SM Yukawa couplings defined in eq. (3.1) read

$$\begin{aligned} 16\pi^2\mu\frac{d}{d\mu}[Y_u]_{ij} &= [Y_u]_{ij}\left(-8g_3^2 - \frac{9}{4}g_2^2 - \frac{17}{20}g_1^2\right) + \mathbf{T}^*[Y_u]_{ij} + [\mathcal{Y}''_{QQ}]_{ik}[Y_u]_{kj} + [Y_u]_{ik}[\mathcal{Y}''_{uu}]_{kj} \\ &\quad - 2\left([Y_d Y_d^\dagger Y_u]_{ij} + [y_2^b Y_e x_2^b]^\dagger_{ij}\right), \end{aligned} \quad (4.32)$$

$$\begin{aligned} 16\pi^2\mu\frac{d}{d\mu}[Y_d]_{ij} &= [Y_d]_{ij}\left(-8g_3^2 - \frac{9}{4}g_2^2 - \frac{1}{4}g_1^2\right) + \mathbf{T}[Y_d]_{ij} + [\mathcal{Y}''_{QQ}]_{ik}[Y_d]_{kj} + [Y_d]_{ik}[\mathcal{Y}''_{dd}]_{kj} \\ &\quad - 2[Y_u Y_u^\dagger Y_d]_{ij}, \end{aligned} \quad (4.33)$$

$$\begin{aligned} 16\pi^2\mu\frac{d}{d\mu}[Y_e]_{ij} &= [Y_e]_{ij}\left(-\frac{9}{4}g_2^2 - \frac{9}{4}g_1^2\right) + \mathbf{T}[Y_e]_{ij} + [\mathcal{Y}''_{LL}]_{ik}[Y_e]_{kj} + [Y_e]_{ik}[\mathcal{Y}''_{ee}]_{kj} \\ &\quad - 2N_c[x_2^b Y_u y_2^b]^\dagger_{ij}. \end{aligned} \quad (4.34)$$

The RGE of the doublet LQ Yukawa couplings defined in eq. (3.7) read

$$\begin{aligned} 16\pi^2\mu\frac{d}{d\mu}[y_2^a]_{ij} &= [y_2^a]_{ij}\left(-4g_3^2 - \frac{9}{4}g_2^2 - \frac{5}{4}g_1^2\right) + \mathbf{T}_2^{ab}[y_2^b]_{ij} + [\mathcal{Y}''_{uu}]_{ik}[y_2^a]_{kj} + [y_2^a]_{ik}[\mathcal{Y}''_{LL}]_{kj} \\ &\quad - 2[Y_e x_2^a Y_u]^\dagger_{ij}, \end{aligned} \quad (4.35)$$

$$\begin{aligned} 16\pi^2\mu\frac{d}{d\mu}[x_2^a]_{ij} &= [x_2^a]_{ij}\left(-4g_3^2 - \frac{9}{4}g_2^2 - \frac{37}{20}g_1^2\right) + \mathbf{T}_2^{ab}[x_2^b]_{ij} + [\mathcal{Y}''_{ee}]_{ik}[x_2^a]_{kj} + [x_2^a]_{ik}[\mathcal{Y}''_{QQ}]_{kj} \\ &\quad - 2[Y_u y_2^a Y_e]^\dagger_{ij}. \end{aligned} \quad (4.36)$$

Finally, the RGE of the triplet LQ Yukawa coupling defined in eq. (3.11) reads

$$16\pi^2\mu\frac{d}{d\mu}[y_3^a]_{ij} = [y_3^a]_{ij}\left(-4g_3^2 - \frac{9}{2}g_2^2 - \frac{1}{2}g_1^2\right) + \mathbf{T}_3^{ab}[y_3^b]_{ij} + [\mathcal{Y}''_{QQ}]_{ik}^*[y_3^a]_{kj} + [y_3^a]_{ik}[\mathcal{Y}''_{LL}]_{kj}. \quad (4.37)$$

5 Phenomenology of fixed point solutions

We have now collected all the necessary ingredients to perform the study of the RGE IR FPs, and to discuss their potential phenomenological implications for the BSM scenarios selected in section 4.2 and 4.3. Our aim is the investigation of solutions to the anomalies in $b \rightarrow s$ and $b \rightarrow c$ transitions with the IR FP values for such couplings.

As anticipated above, we will perform our studies in two distinct scenarios, differentiated by whether the SM sector is extended by (potentially multiple copies of) S_1 and S_3 LQs, or R_2 and S_3 LQs, respectively. In both scenarios we will first study the minimal case, where only one new field involved in $b \rightarrow c$ transitions is considered, namely either S_1^τ or R_2^τ , while two new fields are allowed in the $b \rightarrow s$ sector due to the requirement of a LFU phenomenology, namely S_3^e and S_3^μ . Subsequently, we will also consider the case where 6 NP fields are included in the theory, i.e. three new fields connected to $b \rightarrow c$ transitions, namely either S_1^e , S_1^μ and S_1^τ , or R_2^e , R_2^μ and R_2^τ , and three new fields connected to the $b \rightarrow s$ sector, namely S_3^e , S_3^μ and S_3^τ .

To obtain the FP values for the couplings investigated below, we will employ the following procedure. As a starting point, for each specific SM extension we identify the minimal set of n LQ couplings required to address anomalies in $b \rightarrow s$ and $b \rightarrow c$ transitions; therefore, we take their corresponding n beta functions, which are given for the (S_1, S_3) extension in eqs. (4.25)–(4.27) and for the (R_2, S_3) one in eqs. (4.35)–(4.37), and we consider them in the limit where all the other NP couplings vanish. Finally, we set all the SM couplings entering these beta functions to their experimental values evolved to the scale of 10 TeV, which we choose as the low-energy scale of the RG evolution. We obtain in this way a set of n equations (the beta functions of the LQ couplings of interest are equal to zero) in n variables (the LQ couplings themselves), and the FP values for these couplings are therefore obtained requiring that all equations are fulfilled simultaneously.

Given the non linearity of the system and its high dimensionality, listing all the found solutions goes beyond the scope of our analysis. We will therefore restrict ourselves to reporting phenomenologically interesting FP solutions, namely those that comply with at least one of the following requirements:

- i)* all FP values for the couplings have to be non-vanishing;
- ii)* the S_3^e and S_3^μ couplings have to obey the relation $y_{321}^e y_{331}^e = y_{322}^\mu y_{332}^\mu$, required by the LFU scenario **II** in eq. (2.3);
- iii)* if present, the product of the R_2^τ couplings $y_{223}^\tau x_{233}^{\tau*}$ has to be purely imaginary, in accordance with scenario **C** in eq. (2.10).

Once the couplings are determined by their FP values, the experimental constraints from the anomalies fix the values of the (squared) LQ masses. We will face two possible outcomes: *a)* the FP values for the couplings are large enough to reproduce the desired phenomenology with sufficiently heavy LQ masses, not currently excluded by direct searches at collider. This will also allow us to give a prediction for M_{LQ} , in the case where the low-energy physics is described by the FP values of the LQ couplings; or *b)* the FP values

are not large enough to explain the desired phenomenology, because the LQ are too light to comply with direct searches results.³ Nevertheless, also in this scenario useful conclusions can be drawn: indeed, it will imply that in order to explain $b \rightarrow s$ and $b \rightarrow c$ data, the values for (some of) the LQ couplings is required to be above the FP value. It is therefore interesting to estimate the scale where the Landau pole is induced by such a choice, since this scale can be interpreted as the upper bound for M_{QLU} . We finally remark that for all scenarios discussed below we verified the absence of low-scale Landau poles in the gauge couplings, in agreement with the findings of refs. [47, 67].

5.1 The (S_1, S_3) extension

We start our analysis from the scenario where the SM is extended by one copy of the singlet LQ, S_1^τ , and two copies of the triplet one, S_3^e and S_3^μ . Indeed, as detailed in section 3.1.1 and 3.1.3 respectively, S_1^τ is capable to reproduce the desired low-scale phenomenology for $b \rightarrow c\tau\bar{\nu}$ decays once the couplings y_{133}^τ and x_{123}^τ are non-vanishing, while S_3^e and S_3^μ can produce the correct low-energy effect in $b \rightarrow s\ell^+\ell^-$ transitions when the couplings y_{331}^e , y_{321}^e , y_{332}^μ and y_{322}^μ are allowed. For simplicity, we will assume all couplings to be real.

Aiming at a minimal working example, we set all the other couplings to zero and consider the following structure for the coupling matrices in our analysis:

$$\begin{aligned}
 y_1^\tau &= \begin{pmatrix} 0 & 0 & 0 \\ 0 & 0 & 0 \\ 0 & 0 & y_{133}^\tau \end{pmatrix}, & x_1^\tau &= \begin{pmatrix} 0 & 0 & 0 \\ 0 & 0 & x_{123}^\tau \\ 0 & 0 & 0 \end{pmatrix}, \\
 y_3^e &= \begin{pmatrix} 0 & 0 & 0 \\ y_{321}^e & 0 & 0 \\ y_{331}^e & 0 & 0 \end{pmatrix}, & y_3^\mu &= \begin{pmatrix} 0 & 0 & 0 \\ 0 & y_{322}^\mu & 0 \\ 0 & y_{332}^\mu & 0 \end{pmatrix}.
 \end{aligned} \tag{5.1}$$

The IR FP values for these six non-vanishing couplings are therefore obtained by searching for the simultaneous zeros of their relative beta functions, as given in section 4.2. Only one family of solutions is found to be complying with requirement *i*) listed above, which we report in table 1. The solution is characterized by sign ambiguities, meaning that we can simultaneously flip signs of several couplings to find new solutions: for each of the two S_1^τ couplings both signs are allowed, while for the four S_3^e and S_3^μ couplings an odd number of them, namely either one or three, has to be negative, with the remaining ones being positive. This means that this family of solution is composed by 32 different scenarios, distinguished by sign permutations.

Unfortunately, this family of solutions is phenomenologically non-viable. On the one hand, the S_1^τ sector looks promising, with both couplings being ~ 1 and hence complying with the size implied by $b \rightarrow c$ anomalies and given at eq. (3.6). On the other hand, the S_3^e sector has an unacceptable, albeit intriguing, behaviour: indeed, the couplings are

³A third possibility would consist to ascribe to LQs only a part of the NP contributions required to address the current experimental picture. This scenario would however require to further extend the NP sector to fully explain data, with a consequent modification of the RGE due to the presence of additional degrees of freedom. Such a scenario goes beyond the scope of this paper.

y_{133}^τ	x_{123}^τ	y_{321}^e	y_{331}^e	y_{322}^μ	y_{332}^μ
0.986	0.871	0.672	0.433	0.672	-0.433

Table 1. Values for the IR FP of the six non-vanishing LQ couplings defined in eq. (5.1). Additional solutions obtained via sign permutation are allowed as well, see text for further details.

y_{131}^e	x_{121}^e	y_{132}^μ	x_{122}^μ	y_{133}^τ	x_{123}^τ	y_{321}^e	y_{331}^e	y_{322}^μ	y_{332}^μ	$y_{3,23}^\tau$	y_{333}^τ
0.291	1.006	0.291	1.006	0.291	1.006	0.749	0.172	0.172	0.749	0.664	-0.388
0.291	1.006	0.291	1.006	0.291	1.006	0.172	0.749	0.749	0.171	0.663	-0.388

Table 2. Values for the IR FP of the twelve non-vanishing LQ couplings defined in eq. (5.2). Additional solutions obtained via sign permutation are allowed as well, see text for further details.

connected by the relation $y_{321}^e y_{331}^e = -y_{322}^\mu y_{332}^\mu$, which is in maximal disagreement with requirement *ii*). For this reason, it is not possible to connect the low-energy behaviour of this kind of LQ extension of the SM to the IR FP values of the NP couplings, if trying to address coherently the pattern of deviations in B meson decays.

We therefore move to inspect a more generalized scenario, where six NP fields are allowed in the extension of the SM. In analogy of the three particle scenario, we allow only the following couplings to be non-vanishing:

$$\begin{aligned}
 y_1^e &= \begin{pmatrix} 0 & 0 & 0 \\ 0 & 0 & 0 \\ y_{131}^e & 0 & 0 \end{pmatrix}, & y_1^\mu &= \begin{pmatrix} 0 & 0 & 0 \\ 0 & 0 & 0 \\ 0 & y_{132}^\mu & 0 \end{pmatrix}, & y_1^\tau &= \begin{pmatrix} 0 & 0 & 0 \\ 0 & 0 & 0 \\ 0 & 0 & y_{133}^\tau \end{pmatrix}, \\
 x_1^e &= \begin{pmatrix} 0 & 0 & 0 \\ x_{121}^e & 0 & 0 \\ 0 & 0 & 0 \end{pmatrix}, & x_1^\mu &= \begin{pmatrix} 0 & 0 & 0 \\ 0 & x_{122}^\mu & 0 \\ 0 & 0 & 0 \end{pmatrix}, & x_1^\tau &= \begin{pmatrix} 0 & 0 & 0 \\ 0 & 0 & x_{123}^\tau \\ 0 & 0 & 0 \end{pmatrix}, \\
 y_3^e &= \begin{pmatrix} 0 & 0 & 0 \\ y_{321}^e & 0 & 0 \\ y_{331}^e & 0 & 0 \end{pmatrix}, & y_3^\mu &= \begin{pmatrix} 0 & 0 & 0 \\ 0 & y_{322}^\mu & 0 \\ 0 & y_{332}^\mu & 0 \end{pmatrix}, & y_3^\tau &= \begin{pmatrix} 0 & 0 & 0 \\ 0 & 0 & y_{323}^\tau \\ 0 & 0 & y_{333}^\tau \end{pmatrix}.
 \end{aligned} \tag{5.2}$$

In this new scenario, it is possible to find the following two families of solutions, both complying with requirements *i*) and *ii*). The results are listed in table 2. Similarly to the previous case, also these solutions are characterized by sign ambiguities: concerning the six couplings in the S_1 sector, both signs are allowed for each of them, yielding 64 different configurations; on the other hand, concerning the six couplings in the S_3 sector, the product of the electron couplings and the one of the muon coupling have to share the same sign, while the product of the tau ones have to be opposite, yielding 16 different configurations. Hence, in total, each family of solutions is composed by 1024 distinct solutions due to sign permutations.

It is interesting to highlight that requirement *ii*) is not accidentally fulfilled, but it is met due to the pairs of couplings (y_{321}^e, y_{332}^μ) and (y_{331}^e, y_{322}^μ) sharing the same IR FP, respectively. Hence, the low-energy LFU observed in $b \rightarrow s\ell\ell$ transitions can be elegantly explained due to a dynamical behaviour, with the couplings not having to share the same

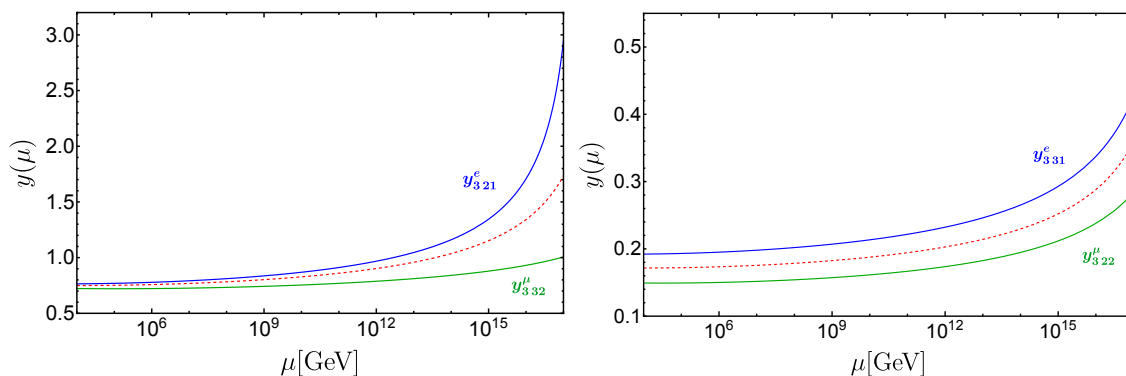


Figure 3. Scenario of eq. (5.2): Left panel: running of the couplings (y_{321}^e and y_{332}^μ) from the high-scale to the low-scale; the FP solution is given in dashed red. Right panel: running of the couplings (y_{331}^e and y_{322}^μ) from the high-scale to the low-scale; the FP solution is given in dashed red.

pattern at the high-scale. An example of this behaviour can be seen in the two panels of figure 3, where the four couplings are taken to be different at the high-scale but are attracted to the same two low-scale values, which corresponds to the FP solution of their beta functions. In particular, the four couplings are evolved from $\mu_h = 10^{17}$ GeV down to $\mu_l = 10^4$ GeV, and their values are reported below:

$$\begin{aligned}
 y_{321}^e(\mu_h) &= 2.95, & y_{332}^\mu(\mu_h) &= 1.00, & y_{331}^e(\mu_h) &= 0.426, & y_{322}^\mu(\mu_h) &= 0.284, \\
 y_{321}^e(\mu_l) &= 0.765, & y_{332}^\mu(\mu_l) &= 0.722, & y_{331}^e(\mu_l) &= 0.192, & y_{322}^\mu(\mu_l) &= 0.149.
 \end{aligned}
 \tag{5.3}$$

Note that the beta functions also depend on SM couplings which depend on the renormalization scale μ . Therefore the FP solution of the LQ couplings is not a constant line.

Employing now the FP values for the LQ couplings and inverting eq. (3.12), one infers the scale for the LQ masses to be

$$M_{S_3^e} = M_{S_3^\mu} = 14.5 \sqrt{\frac{0.04}{|V_{tb}V_{ts}^*|}} \sqrt{\frac{-0.4}{C_L^U}} \text{ TeV}.
 \tag{5.4}$$

It is worthwhile to compare this with the prediction from the UV FP analysis in ref. [68]. As a first remark, no choice of UV boundary conditions can lead to IR values of the LQ couplings with a positive beta function, so that at least one of the two couplings entering the $b \rightarrow s\ell^+\ell^-$ amplitude must be (in magnitude) below its IR fixed point. Indeed, the product of the low-energy values of these couplings found in ref. [68] is smaller than ours, with the larger coupling similar in size to ours. Thus also the corresponding value for $M_{S_3^{e,\mu}}$ inferred from eq. (5.4) is smaller. Eq. (5.4) sets an upper bound on $M_{S_3^{e,\mu}}$ for any choice of UV boundary condition at the GUT or Planck scale. At the same time, any $S_3^{e,\mu}$ discovery with a mass close to the value in eq. (5.4) will imply LQ couplings close to their IR fixed point, so that their high-energy values are unpredictable. The lower bound on the products of the couplings and thereby on $M_{S_3^{e,\mu}}$ found in ref. [68] is much more sensitive to the UV boundary condition, as it results from UV values of couplings too small to ever reach the IR fixed point. In other words: the smaller $M_{S_3^{e,\mu}}$, the more information can be inferred on the UV values of the couplings from low-energy measurements.

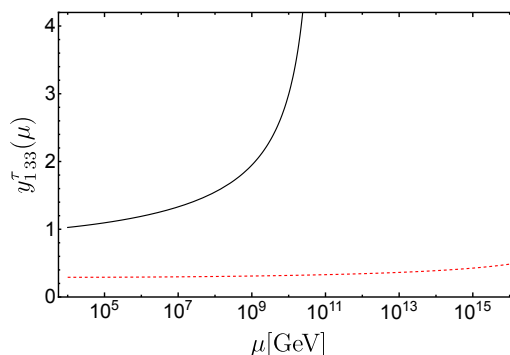


Figure 4. Emergence of a Landau pole in the running of the coupling y_{123}^τ , when a value compatible with $b \rightarrow c\tau\bar{\nu}$ data is assumed at the low-scale. The FP solution is given in dashed red.

It is also interesting to notice that, with these values for the LQ couplings and mass, the expected impact to the $b \rightarrow s\nu\bar{\nu}$ transitions ratio $R_{K^{(*)}}^{\nu\bar{\nu}}$, defined at eq. (2.6) reads $R_{K^{(*)}}^{\nu\bar{\nu}} \simeq 1.1$, hence not large enough to meaningfully also reduce the recent Belle II excess for $R_K^{\nu\bar{\nu}}$ [51].

Finally, the emergence of an electron-muon universality implies also a strong and precise prediction for the tau couplings, whose product is characterized by an opposite sign w.r.t. the light leptons. In particular, both FP solutions predict an enhancement in the tau sector (opposite to the suppression implied by present $b \rightarrow s$ data in light leptons) corresponding to $C_L^\tau(\mu_b) \sim 0.8$, if one assumes $M_{S_3^e} = M_{S_3^\mu} = M_{S_3^\tau}$.

The situation is different in the $b \rightarrow c$ sector: indeed, the FP solution for the S_1^τ coupling yield $y_{133}^\tau x_{123}^\tau \simeq -0.3$, where the freedom on the coupling signs allows us to choose $x_{123}^\tau \simeq -1$; however, when confronting this value with eq. (3.6), in order to address the anomalies in $b \rightarrow c$ transitions S_1^τ would be required to have a mass equal to $M_{S_1^\tau} \sim 0.8$ TeV, value which has already been excluded by direct searches at LHC.⁴ This implies that, if one would like to address the current experimental situation in this sector as well, the value for y_{123}^τ at the low scale $\mu_l = 10^4$ GeV has to be taken well above the FP solution, namely equal to $y_{123}^\tau \sim 1$. In turn, this implies the emergence of a Landau pole at a scale around $\mu \sim 10^{11}$ GeV, which is the scale where y_{123}^τ diverges as can be observed in figure 4.

To conclude we have obtained that, when extending the SM sector with the 6 scalar LQs $S_1^e, S_1^\mu, S_1^\tau, S_3^e, S_3^\mu$ and S_3^τ , thanks to the IR FP behaviours of their couplings it is possible to explain the observed pattern of anomalies in $b \rightarrow s\ell\ell$ transitions by introducing S_3^e and S_3^μ LQs with masses at the ~ 10 TeV scale and arbitrary high-scale couplings; on the other hand, in order to address the experimental picture in $b \rightarrow c\tau\bar{\nu}$ transitions as well, a value above the FP solution is required for one of the couplings, inducing an upper limit to the LQU scale equal to $M_{\text{LQU}} \lesssim 10^{11}$ GeV, which is far below the GUT scale and corroborates ideas of multi-step unification [70].

⁴The NP contribution to $C_{V_L}^{e,\mu}$ coming from non-vanishing couplings of S_1^e and S_1^μ are strongly constrained, see e.g. ref. [29] and references therein. In order to suppress such undesirable effects, the masses of these two LQs are considered to be sensitively heavier than the scale of $M_{S_1^\tau}$.

$y_{2\ 23}^\tau$	$x_{2\ 33}^\tau$	$y_{3\ 21}^e$	$y_{3\ 31}^e$	$y_{3\ 22}^\mu$	$y_{3\ 32}^\mu$
$1.094\ i$	0.783	0.654	0.472	0.654	-0.472
1.094	$0.783\ i$	0.654	0.472	0.654	-0.472

Table 3. Values for the IR FP of the six non-vanishing LQ couplings defined in eq. (5.5). Additional solutions obtained via sign permutation are allowed as well, see text for further details.

5.2 The (R_2, S_3) extension

We move on to the study of the SM extended by one doublet LQ, R_2^τ , and two copies of the triplet one, S_3^e and S_3^μ . Once again, the triplet LQs are employed to obtain the desired low-energy effect in $b \rightarrow s\ell^+\ell^-$ transitions by means of non-vanishing values for the couplings $y_{3\ 31}^e$, $y_{3\ 21}^e$, $y_{3\ 32}^\mu$ and $y_{3\ 22}^\mu$. On the other hand, following now section 3.1.2, we adopt the doublet LQ in order to explain the $b \rightarrow c\tau\bar{\nu}$ decays phenomenology, which require the presence of the $y_{2\ 23}^\tau$ and $x_{2\ 33}^\tau$, with their product being imaginary as detailed in requirement *iii*). We therefore allow the two R_2^τ couplings to be complex.

The minimal set of non-vanishing couplings required by our analysis is therefore:

$$\begin{aligned}
 y_2^\tau &= \begin{pmatrix} 0 & 0 & 0 \\ 0 & 0 & y_{2\ 23}^\tau \\ 0 & 0 & 0 \end{pmatrix}, & x_2^\tau &= \begin{pmatrix} 0 & 0 & 0 \\ 0 & 0 & 0 \\ 0 & 0 & x_{2\ 33}^\tau \end{pmatrix}, \\
 y_3^e &= \begin{pmatrix} 0 & 0 & 0 \\ y_{3\ 21}^e & 0 & 0 \\ y_{3\ 31}^e & 0 & 0 \end{pmatrix}, & y_3^\mu &= \begin{pmatrix} 0 & 0 & 0 \\ 0 & y_{3\ 22}^\mu & 0 \\ 0 & y_{3\ 32}^\mu & 0 \end{pmatrix}.
 \end{aligned} \tag{5.5}$$

In a similar fashion to the previous scenario, we look now for the simultaneous zeros of the couplings beta functions, as given in section 4.3. In this case, two families of solutions are found to be complying with requirements *i*) and *iii*) listed above, identified by which of the two R_2^τ couplings is purely imaginary, and listed in table 3. These solutions are both characterized by the same sign ambiguities: for each of the two R_2^τ couplings both signs are allowed, while for the four S_3^e and S_3^μ couplings an odd number of them, namely either one or three, has to be negative, with the remaining ones being positive. This means that both families of solution are composed by 32 different scenarios each, distinguished by sign permutations.

The minimal scenario is not found to be phenomenologically viable in this configuration as well. A maximal disagreement with requirement *ii*) is again present, with $y_{3\ 21}^e y_{3\ 31}^e = -y_{3\ 22}^\mu y_{3\ 32}^\mu$, invalidating an explanation to $b \rightarrow s\ell^+\ell^-$ data. Moreover, even if requirement *iii*) is fulfilled, the FP values for the R_2^τ couplings are not acceptable if one wants to address anomalies in $b \rightarrow c\tau\bar{\nu}$ transitions: indeed, the product of the two couplings is well below ~ 2 (in modulus), which is the value required to have a mass for the LQ not excluded by direct searches, see section 3.1.2.

We therefore move to inspect a more generalized scenario, where six NP fields are allowed in the extension of the SM. In analogy of the three particle scenario, we allow only

$y_{2\ 21}^e$	$x_{2\ 13}^e$	$y_{2\ 22}^\mu$	$x_{2\ 23}^\mu$	$y_{2\ 23}^\tau$	$x_{2\ 33}^\tau$	$y_{3\ 21}^e$	$y_{3\ 31}^e$	$y_{3\ 22}^\mu$	$y_{3\ 32}^\mu$	$y_{3\ 23}^\tau$	$y_{3\ 33}^\tau$
0.584	0.837	0.584	0.837	$0.584 i$	0.837	0.679	0.181	0.679	0.181	0.521	-0.472
0.584	0.837	0.584	0.837	0.584	$0.837 i$	0.679	0.181	0.679	0.181	0.521	-0.472

Table 4. Values for the IR FP of the twelve non-vanishing LQ couplings defined in eq. (5.6). Additional solutions obtained via sign permutation are allowed as well, see text for further details.

the following couplings to be non-vanishing:

$$\begin{aligned}
 y_2^e &= \begin{pmatrix} 0 & 0 & 0 \\ y_{2\ 21}^e & 0 & 0 \\ 0 & 0 & 0 \end{pmatrix}, & y_2^\mu &= \begin{pmatrix} 0 & 0 & 0 \\ 0 & y_{2\ 22}^\mu & 0 \\ 0 & 0 & 0 \end{pmatrix}, & y_2^\tau &= \begin{pmatrix} 0 & 0 & 0 \\ 0 & 0 & y_{2\ 23}^\tau \\ 0 & 0 & 0 \end{pmatrix}, \\
 x_2^e &= \begin{pmatrix} 0 & 0 & x_{2\ 13}^e \\ 0 & 0 & 0 \\ 0 & 0 & 0 \end{pmatrix}, & x_2^\mu &= \begin{pmatrix} 0 & 0 & 0 \\ 0 & 0 & x_{2\ 23}^\mu \\ 0 & 0 & 0 \end{pmatrix}, & x_2^\tau &= \begin{pmatrix} 0 & 0 & 0 \\ 0 & 0 & 0 \\ 0 & 0 & x_{2\ 33}^\tau \end{pmatrix}, \\
 y_3^e &= \begin{pmatrix} 0 & 0 & 0 \\ y_{3\ 21}^e & 0 & 0 \\ y_{3\ 31}^e & 0 & 0 \end{pmatrix}, & y_3^\mu &= \begin{pmatrix} 0 & 0 & 0 \\ 0 & y_{3\ 22}^\mu & 0 \\ 0 & y_{3\ 32}^\mu & 0 \end{pmatrix}, & y_3^\tau &= \begin{pmatrix} 0 & 0 & 0 \\ 0 & 0 & y_{3\ 23}^\tau \\ 0 & 0 & y_{3\ 33}^\tau \end{pmatrix}.
 \end{aligned} \tag{5.6}$$

We find also in this generalized scenario two families of solution complying with requirements *i*) and *iii*), according to which is the R_2^τ coupling to assume imaginary values. The results are reported in table 4. In a similar fashion to what observed in the previous section, these solutions are characterized by the same sign ambiguities: both signs are allowed for each of the R_2 couplings, yielding 64 different configurations, while the sign has to be the same for the product of both S_3^e and S_3^μ couplings, respectively, and opposite for the product of S_3^τ ones, yielding 16 different configurations. Summarizing, each family of solutions is composed by 1024 distinct solutions due to sign permutations.

These found solutions share a similar phenomenology to the ones found in the general case studied in section 5.1. Indeed, requirement *ii*) is fulfilled since the pairs of couplings $(y_{3\ 21}^e, y_{3\ 32}^\mu)$ and $(y_{3\ 31}^e, y_{3\ 22}^\mu)$ share the same IR FP, respectively: we therefore obtain that, also in this scenario, the low-energy LFU behaviour required to address $b \rightarrow sl^+\ell^-$ data can be ascribed to a FP origin. Moreover, the inferred value from eq. (3.12) for the LQ masses now reads

$$M_{S_3^e} = M_{S_3^\mu} = 14.1 \sqrt{\frac{0.04}{|V_{tb}V_{ts}^*|}} \sqrt{\frac{-0.4}{C_L^U}} \text{ TeV}, \tag{5.7}$$

Finally, the prediction for $R_{K^{(*)}}^{\nu\bar{\nu}}$ defined at eq. (2.6) is equal to $R_{K^{(*)}}^{\nu\bar{\nu}} \simeq 1.1$, again not large enough to significantly reduce the Belle II excess in $R_K^{\nu\bar{\nu}}$ [51]. To conclude, in this scenario as well we observe an opposite behaviour in the tau sector compared to the one observed for the light leptons, with the product of the tau couplings showing again an opposite sign and a prediction for the NP effect in this sector equal to $C_L^T(\mu_b) \sim 0.8$, again in the case of degenerate masses.

On the other hand, the situation in the $b \rightarrow c$ sector is again different: the tau couplings product reads here in both cases $|y_{1\ 33}^\tau x_{1\ 23}^\tau| \simeq 0.5$, again too small to reproduce the desired

y_{321}^e	y_{331}^e	y_{322}^μ	y_{332}^μ
0.622	0.533	0.622	-0.533

Table 5. Values for the IR FP of the four non-vanishing LQ couplings entering in y_3^e and y_3^μ matrices defined in eq. (5.1). Additional solutions obtained via sign permutation are allowed as well, see text for further details.

phenomenology. It is nevertheless interesting to investigate, in this scenario as well, the implications of taking values for the couplings above the FP solution. Indeed, taking for both couplings a value in modulus of the order $\sim \sqrt{2}$, we can observe again the emergence of a Landau pole, found this time at the scale $\mu \sim 10^8$ GeV.

In conclusion, we observed that the study of IR FPs yield interesting phenomenological implications when the SM is extended with the 6 scalar LQs $R_2^e, R_2^\mu, R_3^\tau, S_3^e, S_3^\mu$ and S_3^τ . In particular, the LFU required at the low scale for $b \rightarrow s\ell^+\ell^-$ transitions can be obtained by the FP behaviours of the S_3^e and S_3^μ couplings, whose masses are required to be at the ~ 10 TeV scale while no additional conditions are requested for the coupling values at the high-scale. On the other hand, a value for the R_3^τ couplings is required to be above the FP solution when confronting with $b \rightarrow c\tau\bar{\nu}$, implying the emergence of an upper limit to the LQU scale equal to $M_{\text{LQU}} \lesssim 10^8$ GeV.

5.3 The S_3 extension

We conclude this section by studying the FP solution of SM extensions of S_3 LQs only, even if in this scenario $b \rightarrow c\tau\bar{\nu}$ data cannot be explained. Indeed, motivated by the findings of sections 5.1 and 5.2, it is interesting to investigate whether the dynamical emergence of LFU in the S_3 contributions to $b \rightarrow s\ell^+\ell^-$ transitions arises only in the presence of additional LQs in the theory as well, or it is an exclusive feature of the triplet LQs.

Following the approach of the previous analyses, we start our study from the scenario where only S_3^e and S_3^μ are added to the theory, with non-vanishing values for the couplings $y_{331}^e, y_{321}^e, y_{332}^\mu$ and y_{322}^μ . The only found family of solutions complying with requirement *i*) is given in table 5. These solutions share the same features of the scenarios studied in sections 5.1 and 5.2, when only two copies of the triplet LQ were allowed. In particular, once again an odd number of minus signs is allowed for the four couplings, yielding to 8 different solutions distinguished by sign permutations. Moreover, requirement *ii*) is again not fulfilled, due to the emerging feature $y_{321}^e y_{331}^e = -y_{322}^\mu y_{332}^\mu$.

Moving on to the generalized case where the S_3^τ LQ is included as well, the solutions following requirements *i*) and *ii*) are reported in table 6. Also these solutions are qualitatively similar to the ones studied in the previous sections, when all three copies of S_3 were allowed. Indeed, each family of solutions is characterized by the same sign ambiguity, with the sign for both S_3^e and S_3^μ couplings products having to be the same, respectively, and opposite for S_3^τ one. Moreover, requirement *ii*) is again dynamically fulfilled and the following LQ masses are predicted:

$$M_{S_3^e} = M_{S_3^\mu} = 15.3 \sqrt{\frac{0.04}{|V_{tb}V_{ts}^*|}} \sqrt{\frac{-0.4}{C_L^U}} \text{ TeV}, \quad (5.8)$$

y_{321}^e	y_{331}^e	y_{322}^μ	y_{332}^μ	y_{323}^τ	y_{333}^τ
0.760	0.189	0.191	0.759	0.639	-0.452
0.189	0.760	0.759	0.191	0.639	-0.452

Table 6. Values for the IR FP of the six non-vanishing LQ couplings entering in y_3^e , y_3^μ and y_3^τ matrices defined in eq. (5.2). Additional solutions obtained via sign permutation are allowed as well, see text for further details.

We therefore find that, in order to obtain this feature, the additional presence of singlet or doublet LQs in the theory is not required. It is worth to mention that, if one would employ a different version of requirement *ii*) requesting, e.g., universality among electrons and taus, those two sectors would be the ones having couplings with the same product, with the product of muon ones being different and opposite in sign.

6 Conclusions

In this paper, we studied the implications of RGE effects to LQ couplings to fermions in selected BSM scenarios. A popular way to address the recent discrepancies observed in several observables in the decays $b \rightarrow c\tau\bar{\nu}$ and $b \rightarrow s\ell^+\ell^-$ with $\ell = e, \mu$ consists of extending the SM sectors by means of scalar LQs. In particular, the minimal subset of required new fields includes the presence of triplet LQs S_3^e and S_3^μ , coupled with equal strength to electrons and muons, respectively, and of either the singlet LQ S_1^τ or the doublet LQ R_2^τ coupled to taus. Indeed, the former pair of LQs are required to explain anomalies in $b \rightarrow s\mu^+\mu^-$ without violating the reanalysed results of the LFUV ratios $R_{K^{(*)}} \sim 1$, while the latter LQ is necessary to address anomalies in the $b \rightarrow c\tau\bar{\nu}$ sector.

While these new fields are expected to live at scales between a few and a few tens of TeV, one expects a large mass gap between the scales M_{LQ} and M_{QLU} , the scale where the LQs are generated within a theory of quark-lepton unification, because gauge bosons coupling a quark to a lepton must be very heavy. The presence of this large scale separation therefore implies the possibility that the pattern of values of the LQ Yukawa couplings observed at the B meson decay scale (when employing this kind of SM extensions to address the anomalous data) has a dynamical origin stemming from the infrared behaviour of the RG evolution rather than from symmetry properties. In particular, the possibility of such an explanation of the LFU pattern inferred for the S_3^e and S_3^μ couplings from $R_{K^{(*)}} \sim 1$ is tantalizing. To this end, we studied the IR fixed-point (FP) solutions of the beta functions of the LQ couplings and inspected their phenomenology using low-energy flavour data.

We found interesting phenomenological solutions in several scenarios. In particular, every time that the SM is extended by three triplet LQs coupled each to a specific lepton, namely S_3^e , S_3^μ and S_3^τ , we find IR fixed point solutions for which the product of S_3^e couplings is equal to the one of the S_3^μ couplings, so that electron-muon universality can arise dynamically. Such universality is therefore independent from the values assumed by the couplings at the high scale, as shown in an illustrative example in figure 3, and occurs both when the triplet LQs are the only fields added to the SM, or come together with

either three singlet LQs or three doublet ones, namely S_1^e , S_1^μ and S_1^τ , or R_2^e , R_2^μ and R_2^τ , respectively. Moreover, a prediction for the masses of $S_3^{e,\mu}$ between 14 and 15 TeV is obtained (according to the specific scenario), together with a 10% enhancement in $R_{K^{(*)}}^{\nu\bar{\nu}}$. While LQs with these masses are beyond the reach of current collider searches, such an increase in $R_{K^{(*)}}^{\nu\bar{\nu}}$ is within the reach of the Belle II experiment. Furthermore, electron-muon universality implies an IR FP for the product of S_3^τ couplings with opposite sign, enhancing C_L^τ over $C_L^{e,\mu}$.

A widely studied research line of flavour physics aims at an understanding of quark masses and Yukawa couplings in terms of broken flavour symmetries. Once LQs are included in such a theory of flavour, it is mandatory to address their representations w.r.t. the chosen flavour group (see ref. [71] for a comprehensive study). The experimental result $R_{K^{(*)}} \sim 1$ teaches us that LQs addressing $b \rightarrow s\ell^+\ell^-$ anomalies must come in multiple copies distinguished by the lepton flavour number to avoid dangerously large contributions to $\mu \rightarrow e$ transitions. Their mass matrix (for the first two generations) must be close to the unit matrix to both avoid $\mu \rightarrow e$ transitions emerging from rotations between weak and mass eigenstates and to accommodate $R_{K^{(*)}} \sim 1$ without the tuning of masses against couplings. This suggests that the LQ mass matrix obeys the SU(2) flavour symmetry of the lepton sector exactly. The results of our paper imply that no symmetry model building for the LQ couplings is necessary: if they are close to their IR fixed-points, LFU emerges dynamically. In this case it will be extremely difficult to gain any insight into their high-energy values, because even small uncertainties of the low-energy values inflate to large errors at high scales (see figure 3) making predictive flavour model-building for these couplings impossible.

On the contrary, a dynamical origin has not been found for the couplings required to address anomalies in $b \rightarrow c\tau\bar{\nu}$ decays. Indeed, both in the singlet and in the doublet scenario the IR FP for the relevant couplings have been always found to be below the implied values from low-energy data. Nevertheless, such findings are of phenomenological interest as well, since couplings values above the IR FP imply the emergence of a Landau pole at the scale $\mu \sim 10^{11}$ GeV or $\mu \sim 10^8$ GeV, depending on whether the SM is extended by scalar or doublet LQs, respectively. This scale can therefore be interpreted as an upper limit on M_{QLU} , giving an upper bound on the energy scale where quark-lepton unification should occur.

Acknowledgments

This research was supported by Deutsche Forschungsgemeinschaft (DFG, German Research Foundation) within the Collaborative Research Center *Particle Physics Phenomenology after the Higgs Discovery (P3H)* (project no. 396021762 — TRR 257).

Open Access. This article is distributed under the terms of the Creative Commons Attribution License ([CC-BY 4.0](https://creativecommons.org/licenses/by/4.0/)), which permits any use, distribution and reproduction in any medium, provided the original author(s) and source are credited.

References

- [1] LHCb collaboration, *Differential branching fractions and isospin asymmetries of $B \rightarrow K^{(*)}\mu^+\mu^-$ decays*, *JHEP* **06** (2014) 133 [[arXiv:1403.8044](#)] [[INSPIRE](#)].
- [2] LHCb collaboration, *Angular analysis and differential branching fraction of the decay $B_s^0 \rightarrow \phi\mu^+\mu^-$* , *JHEP* **09** (2015) 179 [[arXiv:1506.08777](#)] [[INSPIRE](#)].
- [3] LHCb collaboration, *Branching Fraction Measurements of the Rare $B_s^0 \rightarrow \phi\mu^+\mu^-$ and $B_s^0 \rightarrow f_2'(1525)\mu^+\mu^-$ Decays*, *Phys. Rev. Lett.* **127** (2021) 151801 [[arXiv:2105.14007](#)] [[INSPIRE](#)].
- [4] A. Khodjamirian, T. Mannel, A.A. Pivovarov and Y.M. Wang, *Charm-loop effect in $B \rightarrow K^{(*)}\ell^+\ell^-$ and $B \rightarrow K^*\gamma$* , *JHEP* **09** (2010) 089 [[arXiv:1006.4945](#)] [[INSPIRE](#)].
- [5] A. Khodjamirian, T. Mannel and Y.M. Wang, *$B \rightarrow K\ell^+\ell^-$ decay at large hadronic recoil*, *JHEP* **02** (2013) 010 [[arXiv:1211.0234](#)] [[INSPIRE](#)].
- [6] LHCb collaboration, *Measurement of Form-Factor-Independent Observables in the Decay $B^0 \rightarrow K^{*0}\mu^+\mu^-$* , *Phys. Rev. Lett.* **111** (2013) 191801 [[arXiv:1308.1707](#)] [[INSPIRE](#)].
- [7] LHCb collaboration, *Angular analysis of the $B^0 \rightarrow K^{*0}\mu^+\mu^-$ decay using 3fb^{-1} of integrated luminosity*, *JHEP* **02** (2016) 104 [[arXiv:1512.04442](#)] [[INSPIRE](#)].
- [8] LHCb collaboration, *Measurement of CP-Averaged Observables in the $B^0 \rightarrow K^{*0}\mu^+\mu^-$ Decay*, *Phys. Rev. Lett.* **125** (2020) 011802 [[arXiv:2003.04831](#)] [[INSPIRE](#)].
- [9] LHCb collaboration, *Angular Analysis of the $B^+ \rightarrow K^{*+}\mu^+\mu^-$ Decay*, *Phys. Rev. Lett.* **126** (2021) 161802 [[arXiv:2012.13241](#)] [[INSPIRE](#)].
- [10] G. Hiller and F. Kruger, *More model-independent analysis of $b \rightarrow s$ processes*, *Phys. Rev. D* **69** (2004) 074020 [[hep-ph/0310219](#)] [[INSPIRE](#)].
- [11] LHCb collaboration, *Test of lepton universality in $b \rightarrow s\ell^+\ell^-$ decays*, *Phys. Rev. Lett.* **131** (2023) 051803 [[arXiv:2212.09152](#)] [[INSPIRE](#)].
- [12] LHCb collaboration, *Measurement of lepton universality parameters in $B^+ \rightarrow K^+\ell^+\ell^-$ and $B^0 \rightarrow K^{*0}\ell^+\ell^-$ decays*, *Phys. Rev. D* **108** (2023) 032002 [[arXiv:2212.09153](#)] [[INSPIRE](#)].
- [13] BABAR collaboration, *Evidence for an excess of $\bar{B} \rightarrow D^{(*)}\tau^-\bar{\nu}_\tau$ decays*, *Phys. Rev. Lett.* **109** (2012) 101802 [[arXiv:1205.5442](#)] [[INSPIRE](#)].
- [14] BELLE collaboration, *Measurement of $\mathcal{R}(D)$ and $\mathcal{R}(D^*)$ with a semileptonic tagging method*, *Phys. Rev. Lett.* **124** (2020) 161803 [[arXiv:1910.05864](#)] [[INSPIRE](#)].
- [15] LHCb collaboration, *Measurement of the ratios of branching fractions $\mathcal{R}(D^*)$ and $\mathcal{R}(D^0)$* , *Phys. Rev. Lett.* **131** (2023) 111802 [[arXiv:2302.02886](#)] [[INSPIRE](#)].
- [16] BELLE collaboration, *Measurement of the branching ratio of $\bar{B} \rightarrow D^{(*)}\tau^-\bar{\nu}_\tau$ relative to $\bar{B} \rightarrow D^{(*)}\ell^-\bar{\nu}_\ell$ decays with hadronic tagging at Belle*, *Phys. Rev. D* **92** (2015) 072014 [[arXiv:1507.03233](#)] [[INSPIRE](#)].
- [17] BELLE collaboration, *Measurement of the branching ratio of $\bar{B}^0 \rightarrow D^{*+}\tau^-\bar{\nu}_\tau$ relative to $\bar{B}^0 \rightarrow D^{*+}\ell^-\bar{\nu}_\ell$ decays with a semileptonic tagging method*, *Phys. Rev. D* **94** (2016) 072007 [[arXiv:1607.07923](#)] [[INSPIRE](#)].
- [18] LHCb collaboration, *Measurement of $\mathcal{R}(D^*)$ with hadronic τ^+ decays at $\sqrt{s} = 13\text{ TeV}$ by the LHCb collaboration*, <https://indico.cern.ch/event/1231797/>.
- [19] HFLAV collaboration, *Averages of b-hadron, c-hadron, and τ -lepton properties as of 2021*, *Phys. Rev. D* **107** (2023) 052008 [[arXiv:2206.07501](#)] [[INSPIRE](#)].

- [20] D. Bigi and P. Gambino, *Revisiting $B \rightarrow D\ell\nu$* , *Phys. Rev. D* **94** (2016) 094008 [[arXiv:1606.08030](#)] [[INSPIRE](#)].
- [21] F.U. Bernlochner, Z. Ligeti, M. Papucci and D.J. Robinson, *Combined analysis of semileptonic B decays to D and D^* : $R(D^{(*)})$, $|V_{cb}|$, and new physics*, *Phys. Rev. D* **95** (2017) 115008 [[arXiv:1703.05330](#)] [*Erratum ibid.* **97** (2018) 059902] [[INSPIRE](#)].
- [22] S. Jaiswal, S. Nandi and S.K. Patra, *Extraction of $|V_{cb}|$ from $B \rightarrow D^{(*)}\ell\nu_\ell$ and the Standard Model predictions of $R(D^{(*)})$* , *JHEP* **12** (2017) 060 [[arXiv:1707.09977](#)] [[INSPIRE](#)].
- [23] P. Gambino, M. Jung and S. Schacht, *The V_{cb} puzzle: An update*, *Phys. Lett. B* **795** (2019) 386 [[arXiv:1905.08209](#)] [[INSPIRE](#)].
- [24] M. Bordone, M. Jung and D. van Dyk, *Theory determination of $\bar{B} \rightarrow D^{(*)}\ell^-\bar{\nu}$ form factors at $\mathcal{O}(1/m_c^2)$* , *Eur. Phys. J. C* **80** (2020) 74 [[arXiv:1908.09398](#)] [[INSPIRE](#)].
- [25] G. Martinelli, S. Simula and L. Vittorio, *$|V_{cb}|$ and $R(D)^{(*)}$ using lattice QCD and unitarity*, *Phys. Rev. D* **105** (2022) 034503 [[arXiv:2105.08674](#)] [[INSPIRE](#)].
- [26] M. Blanke et al., *Impact of polarization observables and $B_c \rightarrow \tau\nu$ on new physics explanations of the $b \rightarrow c\tau\nu$ anomaly*, *Phys. Rev. D* **99** (2019) 075006 [[arXiv:1811.09603](#)] [[INSPIRE](#)].
- [27] M. Blanke, A. Crivellin, T. Kitahara, M. Moscati, U. Nierste and I. Nišandžić, *Addendum to “Impact of polarization observables and $B_c \rightarrow \tau\nu$ on new physics explanations of the $b \rightarrow c\tau\nu$ anomaly”*, *Phys. Rev. D* **100** (2019) 035035 [[arXiv:1905.035035](#)] [[INSPIRE](#)].
- [28] LHCb collaboration, *Observation of the decay $\Lambda_b^0 \rightarrow \Lambda_c^+\tau^-\bar{\nu}_\tau$* , *Phys. Rev. Lett.* **128** (2022) 191803 [[arXiv:2201.03497](#)] [[INSPIRE](#)].
- [29] M. Fedele et al., *Impact of $\Lambda_b \rightarrow \Lambda_c\tau\nu$ measurement on new physics in $b \rightarrow c\ell\nu$ transitions*, *Phys. Rev. D* **107** (2023) 055005 [[arXiv:2211.14172](#)] [[INSPIRE](#)].
- [30] Y. Sakaki, M. Tanaka, A. Tayduganov and R. Watanabe, *Testing leptoquark models in $\bar{B} \rightarrow D^{(*)}\tau\bar{\nu}$* , *Phys. Rev. D* **88** (2013) 094012 [[arXiv:1309.0301](#)] [[INSPIRE](#)].
- [31] G. Hiller and M. Schmaltz, *R_K and future $b \rightarrow s\ell\ell$ physics beyond the standard model opportunities*, *Phys. Rev. D* **90** (2014) 054014 [[arXiv:1408.1627](#)] [[INSPIRE](#)].
- [32] I. Doršner, S. Fajfer, A. Greljo, J.F. Kamenik and N. Košnik, *Physics of leptoquarks in precision experiments and at particle colliders*, *Phys. Rept.* **641** (2016) 1 [[arXiv:1603.04993](#)] [[INSPIRE](#)].
- [33] B. Dumont, K. Nishiwaki and R. Watanabe, *LHC constraints and prospects for S_1 scalar leptoquark explaining the $\bar{B} \rightarrow D^{(*)}\tau\bar{\nu}$ anomaly*, *Phys. Rev. D* **94** (2016) 034001 [[arXiv:1603.05248](#)] [[INSPIRE](#)].
- [34] X.-Q. Li, Y.-D. Yang and X. Zhang, *Revisiting the one leptoquark solution to the $R(D^{(*)})$ anomalies and its phenomenological implications*, *JHEP* **08** (2016) 054 [[arXiv:1605.09308](#)] [[INSPIRE](#)].
- [35] G. Hiller, D. Loose and K. Schönwald, *Leptoquark Flavor Patterns & B Decay Anomalies*, *JHEP* **12** (2016) 027 [[arXiv:1609.08895](#)] [[INSPIRE](#)].
- [36] B. Bhattacharya, A. Datta, J.-P. Guévin, D. London and R. Watanabe, *Simultaneous Explanation of the R_K and $R_{D^{(*)}}$ Puzzles: a Model Analysis*, *JHEP* **01** (2017) 015 [[arXiv:1609.09078](#)] [[INSPIRE](#)].
- [37] C.-H. Chen, T. Nomura and H. Okada, *Excesses of muon $g-2$, $R_{D^{(*)}}$, and R_K in a leptoquark model*, *Phys. Lett. B* **774** (2017) 456 [[arXiv:1703.03251](#)] [[INSPIRE](#)].

- [38] A. Crivellin, D. Müller and T. Ota, *Simultaneous explanation of $R(D^{(*)})$ and $b \rightarrow s\mu^+\mu^-$: the last scalar leptoquarks standing*, *JHEP* **09** (2017) 040 [[arXiv:1703.09226](#)] [[INSPIRE](#)].
- [39] M. Jung and D.M. Straub, *Constraining new physics in $b \rightarrow c\ell\nu$ transitions*, *JHEP* **01** (2019) 009 [[arXiv:1801.01112](#)] [[INSPIRE](#)].
- [40] U. Aydemir, T. Mandal and S. Mitra, *Addressing the $R_{D^{(*)}}$ anomalies with an S_1 leptoquark from SO(10) grand unification*, *Phys. Rev. D* **101** (2020) 015011 [[arXiv:1902.08108](#)] [[INSPIRE](#)].
- [41] O. Popov, M.A. Schmidt and G. White, *R_2 as a single leptoquark solution to $R_{D^{(*)}}$ and $R_{K^{(*)}}$* , *Phys. Rev. D* **100** (2019) 035028 [[arXiv:1905.06339](#)] [[INSPIRE](#)].
- [42] A. Crivellin, D. Müller and F. Saturnino, *Flavor Phenomenology of the Leptoquark Singlet-Triplet Model*, *JHEP* **06** (2020) 020 [[arXiv:1912.04224](#)] [[INSPIRE](#)].
- [43] S. Iguro, M. Takeuchi and R. Watanabe, *Testing leptoquark/EFT in $\bar{B} \rightarrow D^{(*)}l\bar{\nu}$ at the LHC*, *Eur. Phys. J. C* **81** (2021) 406 [[arXiv:2011.02486](#)] [[INSPIRE](#)].
- [44] P. Athron, C. Balázs, D.H.J. Jacob, W. Kotlarski, D. Stöckinger and H. Stöckinger-Kim, *New physics explanations of a_μ in light of the FNAL muon $g - 2$ measurement*, *JHEP* **09** (2021) 080 [[arXiv:2104.03691](#)] [[INSPIRE](#)].
- [45] B. Pendleton and G.G. Ross, *Mass and Mixing Angle Predictions from Infrared Fixed Points*, *Phys. Lett. B* **98** (1981) 291 [[INSPIRE](#)].
- [46] M. Ciuchini, M. Fedele, E. Franco, A. Paul, L. Silvestrini and M. Valli, *Constraints on lepton universality violation from rare B decays*, *Phys. Rev. D* **107** (2023) 055036 [[arXiv:2212.10516](#)] [[INSPIRE](#)].
- [47] A. Greljo, J. Salko, A. Smolkovič and P. Stangl, *Rare b decays meet high-mass Drell-Yan*, *JHEP* **05** (2023) 087 [[arXiv:2212.10497](#)] [[INSPIRE](#)].
- [48] M. Algueró, A. Biswas, B. Capdevila, S. Descotes-Genon, J. Matias and M. Novoa-Brunet, *To $(b)e$ or not to $(b)e$: no electrons at LHCb*, *Eur. Phys. J. C* **83** (2023) 648 [[arXiv:2304.07330](#)] [[INSPIRE](#)].
- [49] A.J. Buras, J. Girrbach-Noe, C. Niehoff and D.M. Straub, *$B \rightarrow K^{(*)}\nu\bar{\nu}$ decays in the Standard Model and beyond*, *JHEP* **02** (2015) 184 [[arXiv:1409.4557](#)] [[INSPIRE](#)].
- [50] BELLE collaboration, *Search for $B \rightarrow h\nu\bar{\nu}$ decays with semileptonic tagging at Belle*, *Phys. Rev. D* **96** (2017) 091101 [[arXiv:1702.03224](#)] [*Addendum ibid.* **97** (2018) 099902] [[INSPIRE](#)].
- [51] BELLE collaboration, *Recent belle ii results on radiative and electroweak penguin decays, at EPS-HEP2023 conference*, Hamburg, Germany (2023), <https://indico.desy.de/event/34916/contributions/146877>.
- [52] BELLE-II collaboration, *The Belle II Physics Book*, *PTEP* **2019** (2019) 123C01 [[arXiv:1808.10567](#)] [*Erratum ibid.* **2020** (2020) 029201] [[INSPIRE](#)].
- [53] W. Buchmuller and D. Wyler, *Effective Lagrangian Analysis of New Interactions and Flavor Conservation*, *Nucl. Phys. B* **268** (1986) 621 [[INSPIRE](#)].
- [54] B. Grzadkowski, M. Iskrzynski, M. Misiak and J. Rosiek, *Dimension-Six Terms in the Standard Model Lagrangian*, *JHEP* **10** (2010) 085 [[arXiv:1008.4884](#)] [[INSPIRE](#)].
- [55] R. Alonso, B. Grinstein and J. Martin Camalich, *SU(2) \times U(1) gauge invariance and the shape of new physics in rare B decays*, *Phys. Rev. Lett.* **113** (2014) 241802 [[arXiv:1407.7044](#)] [[INSPIRE](#)].

- [56] J. Aebischer, A. Crivellin, M. Fael and C. Greub, *Matching of gauge invariant dimension-six operators for $b \rightarrow s$ and $b \rightarrow c$ transitions*, *JHEP* **05** (2016) 037 [[arXiv:1512.02830](#)] [[INSPIRE](#)].
- [57] S. Iguro, T. Kitahara and R. Watanabe, *Global fit to $b \rightarrow c\tau\nu$ anomalies 2022 mid-autumn*, [arXiv:2210.10751](#) [[INSPIRE](#)].
- [58] D. Bečirević, I. Doršner, S. Fajfer, N. Košnik, D.A. Faroughy and O. Sumensari, *Scalar leptoquarks from grand unified theories to accommodate the B -physics anomalies*, *Phys. Rev. D* **98** (2018) 055003 [[arXiv:1806.05689](#)] [[INSPIRE](#)].
- [59] W. Buchmuller, R. Ruckl and D. Wyler, *Leptoquarks in Lepton-Quark Collisions*, *Phys. Lett. B* **191** (1987) 442 [*Erratum ibid.* **448** (1999) 320] [[INSPIRE](#)].
- [60] A. Angelescu, D. Bečirević, D.A. Faroughy and O. Sumensari, *Closing the window on single leptoquark solutions to the B -physics anomalies*, *JHEP* **10** (2018) 183 [[arXiv:1808.08179](#)] [[INSPIRE](#)].
- [61] M. González-Alonso, J. Martin Camalich and K. Mimouni, *Renormalization-group evolution of new physics contributions to (semi)leptonic meson decays*, *Phys. Lett. B* **772** (2017) 777 [[arXiv:1706.00410](#)] [[INSPIRE](#)].
- [62] J. Aebischer, A. Crivellin and C. Greub, *QCD improved matching for semileptonic B decays with leptoquarks*, *Phys. Rev. D* **99** (2019) 055002 [[arXiv:1811.08907](#)] [[INSPIRE](#)].
- [63] A. Angelescu, D. Bečirević, D.A. Faroughy, F. Jaffredo and O. Sumensari, *Single leptoquark solutions to the B -physics anomalies*, *Phys. Rev. D* **104** (2021) 055017 [[arXiv:2103.12504](#)] [[INSPIRE](#)].
- [64] M.E. Machacek and M.T. Vaughn, *Two Loop Renormalization Group Equations in a General Quantum Field Theory. 1. Wave Function Renormalization*, *Nucl. Phys. B* **222** (1983) 83 [[INSPIRE](#)].
- [65] M.E. Machacek and M.T. Vaughn, *Two Loop Renormalization Group Equations in a General Quantum Field Theory. 2. Yukawa Couplings*, *Nucl. Phys. B* **236** (1984) 221 [[INSPIRE](#)].
- [66] S. Banik and A. Crivellin, *Renormalization Group Evolution with Scalar Leptoquarks*, [arXiv:2307.06800](#) [[INSPIRE](#)].
- [67] P. Bandyopadhyay, S. Jangid and A. Karan, *Constraining scalar doublet and triplet leptoquarks with vacuum stability and perturbativity*, *Eur. Phys. J. C* **82** (2022) 516 [[arXiv:2111.03872](#)] [[INSPIRE](#)].
- [68] K. Kowalska, E.M. Sessolo and Y. Yamamoto, *Flavor anomalies from asymptotically safe gravity*, *Eur. Phys. J. C* **81** (2021) 272 [[arXiv:2007.03567](#)] [[INSPIRE](#)].
- [69] D. Marzocca, *Addressing the B -physics anomalies in a fundamental Composite Higgs Model*, *JHEP* **07** (2018) 121 [[arXiv:1803.10972](#)] [[INSPIRE](#)].
- [70] P. Fileviez Perez and M.B. Wise, *Low Scale Quark-Lepton Unification*, *Phys. Rev. D* **88** (2013) 057703 [[arXiv:1307.6213](#)] [[INSPIRE](#)].
- [71] I. de Medeiros Varzielas and G. Hiller, *Clues for flavor from rare lepton and quark decays*, *JHEP* **06** (2015) 072 [[arXiv:1503.01084](#)] [[INSPIRE](#)].